PRELIMINARY STUDY OF THE RATE AND DEGREE OF THERMAL IONIZATION OF ARGON BEHIND SHOCK WAVES

Thesis by

Howard Wong

In Partial Fulfillment of the

Requirements For the Degree of

Aeronautical Engineer

California Institute of Technology

Pasadena, California

1961

ACKNOWLEDGMENT

I am greatly indebted to Professor R. Jahn for the suggestion of the problem and for his continued interest and discussions throughout the course of this work.

ABSTRACT

A microwave system (K-band, 24KMC) was designed and assembled to study the degree of ionization in argon as a function of time or distance behind shock waves in a shock tube. The relaxation time for ionization and the attenuation and reflection of the microwave at equilibrium were measured for Mach numbers from 6.19 to 7.74 at p_1 of 5mm and 10mm Hg to determine the influence of temperature, density, collision cross-section and impurities. These measurements were complemented with theoretical calculation of microwave absorption and electron density at equilibrium for a Mach number range of 6 to 8 with initial pressures P_1 of 1 mm to 10mm Hg.
(Sections II, III, IV)

TABLE OF CONTENTS

I. INTRODUCTION

The present work described is part of a general study of the dynamics of reacting gases. The problems are very complex because of the simultaneous occurrence of non-independent reactions such as excitation, dissociation, ionization and chemical change. The particular phenomena considered here is thermal ionization of the gas. To simplify the problem further a simple gas (argon) is chosen for this study. It is hoped that after attaining a better understanding of the reactions of this gas, the techniques developed can be applied to more complex gas mixtures (i.e. air).

The experiments are all focussed on conditions behind the incident shock wave developed in a shock tube. The mechanism[1] of ionization starts as soon as the shock passes through the gas, setting it in motion and giving the gas a high enthalpy. The gas particles will transfer their translational energy to other degrees of freedom and may eventually bring about excitation and ionization by :-

(a) thermal atom - atom collision

(b) thermal electron - atom collision

(c) photoionization

Which of the above processes will predominate during the non-equilibrium[9] period will depend primarily on the number

density and energy level of the particles and their effective collision cross-sections. Ideally, these factors will completely determine the relaxation time of this process. In practice, one must not neglect the effects of minute amounts of impurities on the rate of ionization even though the contributions of electrons from these impurities does not affect the equilibrium level.

At present measurements of the rate and degree of ionization of gases are hampered by the lack of means to measure them accurately, particularly in regions of low electron density and fast reaction time. The methods and techniques used thus far are reviewed in ref. 2,3. Using microwaves as probes (spatial resolution limited by the wavelength employed) will reduce some of these problems and has the added advantage of not introducing any foreign element into the flow. Microwaves have long been used in the investigation of ionized gases, but only recently have they been used for the study of the properties of plasmas[4,34] generated in shock tubes. In using electromagnetic waves to probe the ionized gas, we are primarily interested in the disturbance (absorption and scatter) of the propagating waves by the gas, rather than the disturbance of the gas by the wave field. This physical situation depends on the strength and frequency of the impressed signal, the free charge and particle densities and whether or not the

atoms and molecules have permanent dipoles. The microwaves (24KMC) used are of such small amplitude that no components of the gas other than the electrons both free and bound are significantly disturbed. Thus the attenuation and reflection of the microwaves in the ionized gas will depend on the collision frequencies of electron and atoms, impressed wave frequency and the plasma frequency in the experimental set-up. The theory derived does not take into account the temperature, pressure, velocity and species gradients near the walls of the shock tube which will add to the complication in the interpretation of our data. See reference (30) for amplification.

The purpose of this paper is a preliminary study in the utilization of microwave technique to determine the rate and degree of thermal ionization of argon behind shock waves generated in a shock tube ($6.19 \leq M \leq 7.74$, $p_1 = 5,10$mm). Only the measurements of overall attenuation (absorption + reflection) of the microwaves at equilibrium conditions behind the incident shocks are compared with theoretical values. The theoretical calculations in the following sections (II, III, IV) contain the equilibrium conditions (temperature, pressure, electron density, attenuation factor) behind the shock waves at various initial pressure conditions.

II. THERMAL IONIZATION IN GASES

Degree of Ionization at Equilibrium. Derivation of Saha Equation.[5]

This equation relates the degree of ionization or electron density to the temperature and pressure at equilibrium conditions, and is independent of the reaction chain by which equilibrium is reached.

The assumptions made in the derivation of the equation for argon are:

(a) Each specie of the system is treated as a perfect gas. That is the body forces between particles are assumed small and have negligible effect on thermal and physical properties of the entire gas. This assumption will hold as long as the density is moderate.

(b) All the neutral atoms are unexcited (error is less than 1% for $T = 15{,}000^{\circ}K$) [8]

(c) The ionized atoms are in two possible states, $^2P_{\frac{3}{2}}$, $^2P_{\frac{1}{2}}$

For a reaction

$$\nu_1 A_1 \rightleftharpoons \nu_2 A_2 + \nu_3 A_3$$

which takes place at constant T and P, the change in the Gibbs function G,

$$dG_{T,P} = 0 \qquad \text{at equilibrium}$$

when $$G = f(T, P, N_1, \ldots N_j)$$

$$dG = -SdT + VdP + \sum_j \mu_j dN_j$$

$\mu_j = \frac{dG}{dN_j}$ - chemical potential of the j constituent of the phase in question

$$G = \Sigma \mu_k N_k = \mu_k'$$

The equation of the reaction at equilibrium is

$$\nu_1 \mu_1 = \nu_2 \mu_2 + \nu_3 \mu_3 \qquad \Delta G = \Delta \mu' = 0$$

$$\mu_k = g_k + RT \ln x_k \tag{1}$$

$$\mu_k = RT(\phi_k + \ln P + \ln x_k) \qquad x_k = \frac{N_k}{N}$$

$$\phi_k = \frac{h_0}{RT} - \frac{1}{R}\int \frac{\int C_p dT}{T^2} dT - \frac{S_0}{R} = f(T)$$

$$\ln \frac{x_2^{\nu_2} x_3^{\nu_3}}{x_1^{\nu_1}} \cdot P^{\nu_3 + \nu_2 - \nu_1} = -(\nu_3 \phi_3 + \nu_2 \phi_2 - \nu_1 \phi_1)$$

The right-hand number is a quantity which is a function only of the temperature and is denoted by ln K, where K is the equilibrium constant

$$\frac{K}{P^{\nu_3 + \nu_2 - \nu_1}} = \frac{x_3^{\nu_3} x_2^{\nu_2}}{x_1^{\nu_1}}$$

Also $\frac{K}{\rho^{\nu_3+\nu_2-\nu_1}} = -\frac{\Delta G}{RT}$ where G is the free energy at p.

To evaluate μ' we shall turn to quantum statistics[6]. The Helmholtz free energy of an assembly of N_i particles

$$F_i = -kT \sum_r \omega_r \ln\left(1 \pm \lambda_i e^{-\epsilon_r/kT}\right)^{\pm 1} + N_i kT \ln \lambda_i$$

λ_i = absolute activity

ω_r = statistical weight

Above equation may be applied to Fermi-Dirac, Bose-Einstein and Maxwell-Boltzmann statistics.

(a) Statistics for classical systems can be derived as limiting case for either Fermi-Dirac or Bose-Einstein formula by assuming $\lambda << 1$.

Then $\lambda_i = \frac{N_i}{f_i(T)}$ N_i = number of particles

$f_i(T)$ = partition function

$$F_i = -N_i kT \left[\ln f_i(T) - \ln N_i + 1\right]$$

This means the number of particles is small compared to the accessible lower energy states. The approximation is adequate as long as the separation between quantal energy levels are small compared with all other energy quantities relevant to the particular problem.

(b) Assume partition function can be given by the products of partition functions of different modes of degree of freedom, i.e. partition functions are still separable factors--can uncouple translational and internal energy.

The partition function for an atom becomes:

$$f_i(T) = \ell_i(T)\, e_i(T)\, n_i(T) = \ell_i(T)\, j_i(T)$$

$$j_i(T) = e_i(T)\, n_i(T)$$

for internal energies (electronic and nuclear) $n_i(T) \cong 1$ for present application.

(c) Interactions between atoms have negligible effect.

(d) No external field except local boundary fields exists.

The chemical potential per particle becomes:

$$\mu_i = \frac{\partial F_i}{\partial N_i} = -kT \ln f_i(T) + kT \ln N_i$$

$$f_i = \frac{(2\pi m_i kT)^{3/2} V j_i(T)}{h^3} \qquad pV = NkT$$

$$f_i = \frac{(2\pi m_i)^{3/2} (kT)^{5/2} N j_i(T)}{p h^3}$$

$$\mu_i = -kT \ln \frac{(2\pi m_i)^{3/2} (kT)^{5/2} j_i(T)}{p h^3} + kT \ln \frac{N_i}{N}$$

$$\mu_i = -kT \ln \frac{(2\pi m_i)^{3/2} (kT)^{5/2} j_i(T)}{p h^3} + kT \ln \frac{p_i}{p}$$

Chemical potential for N_i particles.

$$\mu_i' = -N_i kT \ln \frac{(2\pi m_i)^{3/2} (kT)^{5/2} j_i(T)}{p h^3} + N_i kT \ln \frac{p_i}{p}$$

$$\frac{\mu_i'}{RT} = -n_i \ln \frac{(2\pi m_i)^{3/2}(kT)^{5/2} j_i(T)}{ph^3} + n_i \ln \frac{N_i}{N}$$

At equilibrium

$$\Delta G = \Delta\mu' = 0$$

For the reaction - ionization of argon

$$A \rightleftarrows A^+ + e^-$$

$$\Delta\mu' = 0 \qquad n_{A^+} \ln \frac{N_{A^+}}{N} + n_e \ln \frac{N_e}{N} - n_A \ln \frac{N_A}{N} = n_{A^+} \ln \frac{(2\pi m_{A^+})^{3/2}(kT)^{5/2}}{ph^3}$$

$$+ n_{A^+} \ln j_{A^+}(T) + n_e \ln \frac{(2\pi m_e)^{3/2}(kT)^{5/2}}{ph^3} + n_e \ln j_e(T)$$

$$- n_A \ln \frac{(2\pi m_A)^{3/2}(kT)^{5/2}}{ph^3} - n_A \ln j_A(T)$$

For

$$m_{A^+} = m_A \qquad n_{A^+} = n_e = n_A = 1$$

$$\ln \frac{(2\pi m_e)^{3/2}(kT)^{5/2}}{ph^3} + \ln \frac{j_{A^+}(T) j_e(T)}{j_A(T)} = \ln \left(\frac{N_{A^+}}{N}\right)\left(\frac{N_e}{N}\right)\left(\frac{N}{N_A}\right)$$

Let α = degree of ionization

$$\frac{N_{A^+}}{N} = \frac{\alpha}{1+\alpha} \qquad \frac{N_e}{N} = \frac{\alpha}{1+\alpha} \qquad \frac{N_A}{N} = \frac{1-\alpha}{1+\alpha}$$

$$\frac{\alpha^2}{1-\alpha^2} = \frac{(2\pi m_e)^{3/2}(kT)^{5/2}}{ph^3}\left[\frac{j_{A^+}(T) j_e(T)}{j_A(T)}\right]$$

j_A^+ (T) is the internal partition function for the ionized atom. For the rare gas ions the lowest lying levels are $^2P_{3/2}$, $^2P_{1/2}$ with a small energy difference E_1 between

levels with different J values

$$j_{A^+}(T) = 4 + 2e^{-\frac{E_1}{kT}} \qquad \frac{E_1}{k} = 2060\,^{\circ}K$$

Assume $j_A(T) = 1$. Since we are considering the zero ground state as those electrons bound to the atoms, the free electrons are at an energy state of I, with a weight factor of 2 to account for the spin of $\pm \frac{1}{2}$.

$$j_e(T) = U_0 e^{-\frac{E_0}{kT}} = 2e^{-\frac{I}{kT}} \qquad U_0 = 2$$

$E_0 = I$ = ionization potential = 15.7 ev.

The Saha equation is

$$\frac{\alpha^2}{1-\alpha^2} = \frac{(2\pi m_e)^{3/2}(kT)^{5/2}}{ph^3}(4 + 2e^{-\frac{E_1}{kT}})2e^{-\frac{I}{kT}}$$

$$\alpha = \left[\frac{p}{T^{5/2}} \frac{10^4}{(2 + e^{-\frac{2060}{T}})} e^{\frac{182,000}{T}} + 1\right]^{-\frac{1}{2}} \qquad \begin{matrix} p - cm\ Hg \\ T - {}^{\circ}K \end{matrix}$$

Electron density (electrons/cm^3)

$$n_e = \frac{\alpha}{1+\alpha} \frac{pN_0}{RT}$$

$$n_e = .972 \times 10^{19} \frac{\alpha}{1+\alpha} \frac{p}{T}$$

N_0 = Avogadro No.

p = mm Hg

T = $^{\circ}K$

R = 8.31×10^7 $\frac{ergs}{mode\ ^{\circ}K}$

III. SHOCK TUBE RELATIONS

The process of ionization is initiated by the passage of the shock front through the gas. Figure (21) shows a schematic drawing of the shock tube before and during a run. A diaphragm separates the high pressure chamber (4, filled with helium) and the low pressure chamber (1, filled with argon). When the diaphragm fractures a series of waves progresses downstream through the gas. The local velocity of sound for these waves is no longer constant. For a particular class of solution of the one-dimensional gas equation

$$p = p(\rho) \qquad u = u(\rho)$$

The wave speed is given by

$$c = a_1 + \frac{\gamma+1}{2} u$$

$$c = a_1 \left\{ 1 + \frac{\gamma+1}{\gamma-1} \left[\left(\frac{\rho}{\rho_1} \right)^{\frac{\gamma-1}{2}} - 1 \right] \right\}$$

a_1 - speed of sound in undisturbed fluid

u - particle or gas velocity

Thus from the above equation the wave speed is higher than a_1 in regions of condensation ($\rho > \rho_1$) and lower than a_1 in regions of rarefaction. This means the wave distorts as it propagates, the net effect is to steepen the compression regions and to flatten the expansion regions. The compression wave steepens and reaches an equilibrium state, balanced

by the viscous stresses and pressure forces, a few diameters of tube from the diaphragm. It is then a shock wave. On the other hand, a family of expansion waves propagates into regions (4) and will always remain isentropic for they tend to flatten and so further reduce the velocity and temperature gradients.

Following the shock wave is the contact surface or cold front which acts like a piston surface and also separates the two gases ahead and behind the diaphragm. The pressure and velocity is continuous across the surface but the density is not, assuming negligible diffusion between the gases.

The assumptions made in the derivation of the shock relations are:

(1) heat losses and wall friction (viscous effects) are neglected,

(2) each species of the gas is treated as perfect.

For the case of no ionization, the conditions behind the incident and reflected shock are given in ref. (7) The following will contain the derivation of equilibrium conditions (temperature, density, pressure) behind the incident and reflected shock waves.

Conditions behind Incident Shock with Ionization[8]

(1) $\rho_1 u_1 = \rho_2 u_2$

(2) $p_1 + \rho_1 u_1^2 = p_2 + \rho_2 u_2^2$

(3) $h_1 + \frac{u_1^2}{2} = h_2 + \frac{u_2^2}{2}$

(4) $h = e + \frac{p}{\rho} = \frac{5}{2}(1+\alpha)RT + \alpha R\Theta + \alpha R\beta$

Θ = ionization potential ($^\circ$K)

β = excitation energy of argon ion ($^\circ$K)

(5) $\alpha = \left[\frac{p}{T^{5/2}} \frac{10^4}{(2 + e^{-\frac{2060}{T}})} e^{\frac{182,000}{T}} + 1 \right]^{-\frac{1}{2}}$

(6) $p = \rho(1+\alpha)RT$

In the calculation of the enthalpy of the ionized gas we have neglected excitation energies (β) of the particles. Thus the resulting formulae would be valid only for temperatures less than 16,000°K.

Equations (1) and (2)

$$u_2^2 = \frac{(p_2 - p_1)}{(\rho_2 - \rho_1)} \frac{\rho_1}{\rho_2}$$

$$u_1^2 = \frac{\rho_2}{\rho_1} \frac{(p_2 - p_1)}{(\rho_2 - \rho_1)}$$

Substitute into (3)

(7) $h_2 - h_1 = \frac{1}{2}(p_2 - p_1)\left(\frac{1}{\rho_1} + \frac{1}{\rho_2}\right)$

Substitute in (4)

$$(8)\quad \frac{\rho_2}{\rho_1} = \frac{1 + 4\frac{p_2}{p_1}}{4 + \frac{p_2}{p_1} - \frac{2(\alpha_2 - \alpha_1)}{1+\alpha_1}\frac{\theta}{T_1}}$$

Relative to shock

$$(9)\quad \frac{u_2}{a_1} = M_s\left(1 - \frac{1}{\eta}\right) \qquad \eta = \frac{\rho_2}{\rho_1}$$

$$(10)\quad \frac{p_2}{p_1} = 1 + \gamma_1 M_s^2\left(\frac{\eta - 1}{\eta}\right)$$

$$(11)\quad \frac{h_2}{h_1} = 1 + \frac{\gamma_1 - 1}{2} M_s^2\left(1 - \frac{1}{\eta^2}\right)$$

Combining equations (10) and (8)

$$\frac{p_2}{p_1} = 1 + \gamma_1 M_s^2\left[1 - \frac{4 + \frac{p_2}{p_1} - 2\alpha_2\frac{\theta}{T_1}}{1 + 4\frac{p_2}{p_1}}\right]$$

$$\left(\frac{p_2}{p_1}\right)^2 - \frac{p_2}{p_1}\left(\frac{3}{4} + \frac{3}{4}\gamma_1 M_s^2\right) - \left(\frac{1}{4} - \frac{3}{4}\gamma_1 M_s^2 + \frac{1}{2}\gamma_1\alpha_2 M_s^2\frac{\theta}{T_1}\right) = 0$$

$$\gamma_1 = \frac{5}{3} \qquad \frac{p_2}{p_1} = \frac{1}{\gamma_1}\left[3 + 5M_s^2 + 5\sqrt{(M_s^2 - 1)^2 + \frac{32}{15}\alpha_2\frac{\theta}{T_1}M_s^2}\right]$$

$$\theta = 182{,}000\ ^\circ K\ (15.7\ eV), \qquad T_1 = 300\ ^\circ K$$

For shock wave moving into a non-ionized region ($\alpha_1 = 0$)

(a) Density Ratio

$$\frac{\rho_2}{\rho_1} = \frac{1 + 4\frac{p_2}{p_1}}{4 + \frac{p_2}{p_1} - 2\alpha_2\frac{\theta}{T_1}}$$

(b) Pressure Ratio

$$\frac{p_2}{p_1} = \frac{1}{\gamma_1}\left[3 + 5M_s^2 + 5\sqrt{(M_s^2 - 1)^2 + \frac{32}{15}\alpha_2\frac{\theta}{T_1}M_s^2}\right]$$

(c) Temperature Ratio

$$\frac{T_2}{T_1} = \frac{\rho_1}{\rho_2}\frac{p_2}{p_1}\left(\frac{1}{1+\alpha_2}\right)$$

(d) Degree of Ionization

$$\alpha_2' = \left[\frac{p_2}{T_2^{5/2}}\frac{10^{\alpha}}{(2+e^{-\frac{2060}{T_2}})}e^{\frac{183,000}{T_2}}+1\right]^{-\frac{1}{2}}$$

Solution of Iterative Procedure

(1) For particular Mach number M_s, pressure p_1, temperature T_1, assume an α_2.

(2) Compute $\frac{p_2}{p_1}$, $\frac{T_2}{T_1}$, $\frac{\rho_2}{\rho_1}$, α_2'

(3) If the value of α_2' does not agree with α_2 to four significant figures, recompute α_2' using a new α_2 = original $\alpha_2 + \frac{|\alpha_2 - \alpha_2'|}{3}$

(4) When the values of α agree, use this value of α_2' for the initial guess of the next Mach number

The iterative procedure was first computed using the slide rule to check out the accuracy of equations and rate of convergence. Values used in the computations were obtained by using IBM 709 at the computing center of the University of California at Los Angeles. The maximum number of iterative steps programmed for was 100, but usually less than 30 steps were necessary (figures 1 - 5).

Ionization behind Reflected Shock

(1) $\frac{u_R}{u_s} = \frac{\eta - 1}{\psi - \eta}$ $\qquad \psi = \frac{\rho_s}{\rho_1}, \quad \eta = \frac{\rho_R}{\rho_1}$

(2) $\frac{\rho_s}{\rho_1} = 1 + \gamma_1 M_s^2 \frac{(\eta - 1)}{(\psi - \eta)} (\psi - 1)$

(3) $\frac{h_s}{h_1} = \frac{\frac{5}{2}(1 + \alpha_s) R T_s + \alpha_s R \Theta}{\frac{5}{2} R T_1} = \frac{T_s}{T_1}$

(4) $\frac{h_s}{h_1} = 1 + (\gamma_1 - 1) M_s^2 \left(\frac{\eta - 1}{\eta} \frac{\psi - 1}{\psi - \eta} \right)$

(5) $\alpha_s' = \left[\frac{\rho_s}{T_s^{5/2}} \frac{10^4}{(2 + e^{-\frac{3060}{T_s}})} e^{\frac{183,000}{T_s}} + 1 \right]^{-\frac{1}{2}}$

(6) $\frac{T_s}{T_1} = \frac{\rho_s}{\rho_1} \left(\frac{\rho_1}{\rho_s} \right) \frac{1}{1 + \alpha_s}$

Equate (3) and (4)

(7) $\frac{T_s}{T_1} = \frac{1}{(1 + \alpha_s)} \left[1 + (\gamma_1 - 1) M_s^2 \frac{\eta - 1}{\eta} \left(\frac{\psi - 1}{\psi - \eta} \right) \right] - \frac{2}{5} \frac{\alpha_s \Theta}{(1 + \alpha_s) T_1}$

Equate (6) and (7)

(8) $\alpha_s = \frac{5}{2} \frac{T_1}{\Theta} \left[1 - \frac{\rho_s / \rho_1}{\psi} + (\gamma_1 - 1) M_s^2 \frac{(\eta - 1)}{\eta} \frac{\psi - 1}{\psi - \eta} \right]$

---

(1) $\frac{u_R}{u_s} = \frac{\eta - 1}{\psi - \eta}$

(2) $\frac{\rho_s}{\rho_1} = 1 + \frac{5}{3} M_s^2 \frac{(\eta - 1)}{(\psi - \eta)} (\psi - 1)$

(8) $$\alpha_s = \frac{\xi}{2}\frac{T_1}{\Theta}\left[1 - \frac{P_s/P_1}{\xi} + (\gamma_1 - 1)M_s^2\frac{\gamma-1}{\gamma}\frac{\xi-1}{\xi-\eta}\right]$$

(7) $$\frac{T_s}{T_1} = \frac{P_s/P_1}{\xi}\frac{1}{(1+\alpha_s)}$$

(5) $$\alpha_s' = \left[\frac{P_s}{T_s^{5/2}}\frac{10^4}{(2+e^{-\frac{2010}{T_s}})}e^{\frac{182,000}{T_s}} + 1\right]^{-\frac{1}{2}}$$

Iterative process:

(a) Guess a value of $\frac{\rho_s}{\rho_1} = \xi$.

(b) Compute $\frac{P_s}{\rho_1}$, α_s , $\frac{T_s}{T_1}$, α_s' .

(c) If value of α_s' does not agree with α_s to four significant figures, recompute for a second guess for $\frac{\rho_s}{\rho_1}$.

(d) When the values of α agree use the value of $\frac{\rho_s}{\rho_1}$ for the initial guess of the next Mach number.

This process was done also on the I.B.M. 709. See figures (6-10)

The graphs show the differences between the pressure, temperature and density conditions with and without ionization. With ionization the pressure and density are increased, whereas the temperature is decreased as a result of an increase in the number density of particles present. These effects are not appreciable until the temperature conditions are greater than 5000°K.

Transformation of Time Scale

The time scale we measure in is the laboratory system. The time which we are interested in is the time relative to the shock wave. The conversion can be made easily by observing the x - t diagram.

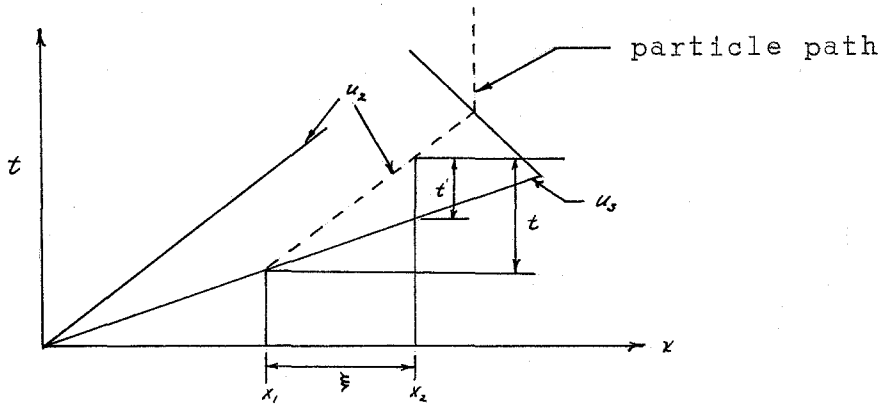

A fluid particle is stationary in x_1 and as the shock passes the fluid particle is set into motion with velocity u_2. We (laboratory system) are observing the process at position x_2. and the time we measured is t . The time relative to the shock is t and the fluid element has travelled a distance before we observe it.

$$\xi = (t - t')u_s = t u_2$$

$$\frac{u_2}{u_s} = \frac{t - t'}{t} = 1 - \frac{t'}{t}$$

$$\frac{t'}{t} = 1 - \frac{u_2}{u_s}$$

From continuity equation

$$\frac{\rho_1}{\rho_2} = 1 - \frac{u_2}{u_s}$$

$$t = \frac{\rho_2}{\rho_1} t'$$

The fluid particle is stationary behind the reflected shock and hence $t = t^1$ in that case.

IV. ELECTROMAGNETIC THEORY

(a) Derivation of the attenuation factor β

In order to determine the attenuation factor of the electric and magnetic vectors of the impressed field, it is necessary to obtain the velocity distribution of the electrons. This velocity distribution can be obtained by an overall solution of Boltzmann's equation.[31] However for the case of roughly constant mean free path an approximate equation where the collision integral is replaced by a collision force is quite adequate. In addition the following assumptions are made:

(a) the ionized medium is isotropic and changing with time.

(b) the electromagnetic waves propagating into the medium are plane-polorized, harmonic time dependent.

Force on the average electron

$$\vec{F}_e = \vec{f}_E + \vec{f}_M + \vec{f}_c$$

Electric force

$$\vec{f}_E = q\vec{E}$$

Magnetic force

$$\vec{f}_M = q\vec{v} \times \vec{B}$$

Damping or collision force

$$\vec{f}_c = -m\nu_c\vec{v}$$

ν_c is the collision frequency and its evaluation is given in part (b) of this section.

$$q\vec{E} + q\vec{v}\times\vec{B} - m\nu_c\vec{v} = m\frac{d\vec{v}}{dt}$$

Maxwell's Equations

$$\nabla\times\vec{E} = -\mu\frac{\partial\vec{H}}{\partial t}$$

$$\nabla\times\vec{H} = \vec{J}_T = \vec{J}_c + \epsilon_0\frac{\partial\vec{E}}{\partial t} = \epsilon\frac{\partial\vec{E}}{\partial t}$$

J_c = convection current due to electrons.

$$\nabla\cdot\vec{D} = 0 \qquad \vec{D} = \epsilon_0\vec{E}$$

$$\nabla\cdot\vec{B} = 0 \qquad \vec{B} = \mu\vec{H}$$

Thus solution of these equations for wave motions will be

$$\nabla^2\vec{E} = \mu\epsilon\frac{\partial^2\vec{E}}{\partial t^2}$$

$$\nabla^2\vec{H} = \mu\epsilon\frac{\partial^2\vec{H}}{\partial t^2}$$

$$\vec{E} = E_0 e^{-i(\omega t - k^* z)} \qquad \vec{H} = H_0 e^{-i(\omega t - k^* z)}$$

Since E and H are harmonic time dependent

$$\nabla\times\vec{E} = i\mu\omega\vec{H}$$

$$\nabla\times\vec{H} = -i\omega\epsilon\vec{E}$$

Maxwell's equations possess certain symmetry in $\vec{E}$, $\vec{H}$; thus $\vec{e}_i\times\vec{E} = \sqrt{\frac{\mu}{\epsilon}}\vec{H}$ $\vec{e}_i$ - direction of propagation

$\mu\epsilon = \frac{1}{u^2}$ u - phase velocity

The relative size of the magnetic and electric forces on a moving charge is

$$\frac{F_M}{F_E} \sim \frac{qv\mu H}{qE} = v\mu\sqrt{\frac{\epsilon}{\mu}} = \frac{v}{u} << 1$$

For our problem we may neglect the effect of the magnetic force. Consistent with the above approximation we can assume μ is a scalar and is equal to μ_0 .

The equation of force now becomes

$$q\vec{E} - m\nu_c\vec{v} = m\frac{d\vec{v}}{dt}$$

Differentiate with respect to time (two times)

$$\frac{d^3\vec{v}}{dt^3} = \frac{q}{m}\frac{d^2\vec{E}}{dt^2} - m\nu_c\frac{d^2\vec{v}}{dt^2}$$

Assume harmonic time dependence for $\vec{E}$ and $\vec{v}$

$$i\omega^3\vec{v} = -i\omega^2\frac{q}{m}\vec{E} + \nu_c\omega^2\vec{v}$$

$$\vec{v} = -\frac{\omega^2\left(\frac{q}{m}\right)\vec{E}}{(i\omega^3 - \nu_c\omega^2)}$$

The convection current due to electrons is

$$\vec{J}_c = nq\vec{v}$$

$$\vec{J}_c = \frac{i\omega\omega_p^2\epsilon_0\vec{E}}{(\omega^2 + i\nu_c\omega)} \qquad \omega_p^2 = \frac{nq^2}{m\epsilon_0} \text{ - plasma frequency.}$$

The total current is equal to the convection plus the displacement current.

$$\vec{J}_T = \vec{J}_c - i\omega\epsilon_0\vec{E} = -i\omega\epsilon_0\vec{E}\left[1 - \frac{\omega_p^2}{\omega^2 + i\nu_c\omega}\right]$$

$$\vec{J}_T = -i\omega\epsilon_0\vec{E}\left[1 - \frac{\omega_p^2}{\omega^2 + i\nu_c\omega}\right]$$

$$\vec{J}_x = -i\omega\epsilon_0\left[1 - \frac{\omega_p^2}{\omega^2 + i\nu_c\omega}\right]\vec{E}_x$$

$$\vec{J}_y = -i\omega\epsilon_0\left[1 - \frac{\omega_p^2}{\omega^2 + i\nu_c\omega}\right]\vec{E}_y$$

$$\vec{J}_z = -i\omega\epsilon_0\left[1 - \frac{\omega_p^2}{\omega^2 + i\nu_c\omega}\right]\vec{E}_z$$

The dielectric constant of the gas is a complex scalar.

$$\epsilon = \epsilon_0\left[1 - \frac{\omega_p^2}{\omega^2 + i\nu_c\omega}\right]$$

The electric field is given by

$$\vec{E} = E_0\, e^{i(\omega t - k^* z)}$$

where

$$k^* = \frac{2\pi}{\lambda} = \frac{\omega}{u} = \omega\sqrt{\mu\epsilon} = \omega\sqrt{\mu_0\epsilon_0\left(1 - \frac{\omega_p^2}{\omega^2 + i\nu_c\omega}\right)}$$

$$k^* = \frac{\omega}{c}\sqrt{1 - \frac{\omega_p^2}{\omega^2 + i\nu_c\omega}} \qquad c = \frac{1}{\sqrt{\mu_0\epsilon_0}}$$

The propagation constant k^* is a complex quantity.

$$k^* = \alpha + i\beta \qquad k^{*2} = \alpha^2 - \beta^2 + 2i\alpha\beta$$

$$\alpha^2 - \beta^2 = \left(\frac{\omega}{c}\right)^2\left[1 - \frac{\omega_p^2\omega^2}{\omega^4 + \nu_c^2\omega^2}\right]$$

$$2\alpha\beta = \left(\frac{\omega}{c}\right)^2\frac{\omega_p^2\nu_c\omega}{\omega^4 + \nu_c^2\omega^2}$$

$$\beta^4 + \left(\frac{\omega}{c}\right)^2\left[1 - \frac{\omega_p^2}{\omega^2 + \nu_c^2}\right]\beta^2 - \frac{1}{4}\left(\frac{\omega}{c}\right)^4\frac{\omega_p^4\nu_c^2\omega^2}{(\omega^4 + \nu_c^2\omega^2)^2} = 0$$

$$\beta^2 = \frac{1}{2}\left(\frac{\omega}{c}\right)^2\left[-\left(1-\frac{\omega_p^2}{\omega^2+\nu_c^2}\right)+\left\{\left(1-\frac{\omega_p^2}{\omega^2+\nu_c^2}\right)^2+\left(\frac{\nu_c}{\omega}\right)^2\left(\frac{\omega_p^2}{\omega^2+\nu_c^2}\right)^2\right\}^{\frac{1}{2}}\right]$$

$$\alpha = \frac{1}{2}\left(\frac{\omega}{c}\right)^2 \frac{\omega_p^2 \omega \nu_c}{\omega^4+\nu_c^2\omega^2}\,\frac{1}{\beta}$$

$$\alpha^2 = \frac{1}{2}\left(\frac{\omega}{c}\right)^2\left[\left(1-\frac{\omega_p^2}{\omega^2+\nu_c^2}\right)+\left\{\left(1-\frac{\omega_p^2}{\omega^2+\nu_c^2}\right)^2+\left(\frac{\nu_c}{\omega}\right)^2\left(\frac{\omega_p^2}{\omega^2+\nu_c^2}\right)^2\right\}^{\frac{1}{2}}\right]$$

The electric field is given by

$$\vec{E} = E_0 e^{-\beta z} e^{i(\omega t - \alpha z)}$$

β is the attenuation coefficient.

Applied to the experiment where we considered only plane transverse electromagnetic wave (tem) being emitted from the microwave apparatus, we need only consider attenuation of the electric field in the z - direction

Using the alternative method of ref. (27) we can write the current in terms of a complex conductivity.

$$\vec{J_e} = (\sigma_r + i\sigma_i)\vec{E}$$

current is not in phase with field.

$$\sigma_r + i\sigma_i = -i\omega\epsilon_0\left[\frac{\omega_p^2}{\omega^2 + i\nu_c\omega}\right]$$

$$\sigma_r + i\sigma_i = i\epsilon_0\omega\left[\frac{\omega_p^2}{\omega^2 + \nu_c^2}\right] + \frac{\epsilon_0\nu_c\omega_p^2}{\omega^2 + \nu_c^2}$$

$$\frac{\sigma_i}{\sigma_r} = \frac{\omega}{\nu_c}$$

$\sigma_r = \dfrac{\epsilon_0\nu_c\omega_p^2}{\omega^2 + \nu_c^2}$ ohmic type behaviour of the medium

$\sigma_i = \dfrac{\epsilon_0\omega\omega_p^2}{\omega^2 + \nu_c^2}$ free electron type behaviour of the medium

$$\left|\frac{E}{E_0}\right| = e^{-\beta z}$$

where

$$\beta^2 = \frac{1}{2}\left(\frac{\omega}{c}\right)^2\left[-\left(1 - \frac{\sigma_i}{\epsilon_0\omega}\right) + \left\{\left(1 - \frac{\sigma_i}{\epsilon_0\omega}\right)^2 + \left(\frac{\sigma_r}{\epsilon_0\omega}\right)^2\right\}^{\frac{1}{2}}\right]$$

Let

$$\frac{\sigma_i}{\epsilon_0\omega} = \frac{\left(\frac{\omega_p}{\omega}\right)^2}{1 + \left(\frac{\nu_c}{\omega}\right)^2} = a$$

$$\frac{\sigma_r}{\epsilon_0\omega} = \frac{\nu_c}{\omega}\left[\frac{\left(\frac{\omega_p}{\omega}\right)^2}{1 + \left(\frac{\nu_c}{\omega}\right)^2}\right] = b = \frac{\nu_c}{\omega}a$$

$$\beta^2 = \frac{1}{2}\left(\frac{\omega}{c}\right)^2\left[-(1-a) + \left\{(1-a)^2 + b^2\right\}^{\frac{1}{2}}\right]$$

The approximate value for small values of $b^2 \ll 1$,

collision frequency is small

$$\beta^2 = \frac{1}{2}\left(\frac{\omega}{c}\right)^2\left[-(1-a) + (1-a)\left\{1 + \frac{b^2}{(1-a)^2}\right\}^{\frac{1}{2}}\right]$$

$$\beta^2 \simeq \frac{1}{2}\left(\frac{\omega}{c}\right)^2\left[\frac{1}{2}\frac{b^2}{(1-a)}\right]$$

$$\beta \simeq \frac{1}{2}\left(\frac{\omega}{c}\right)\frac{\left(\frac{\sigma_r}{\epsilon\omega}\right)}{\left(1-\frac{\sigma_i}{\epsilon\omega}\right)^{\frac{1}{2}}}$$

$$\beta \simeq \frac{1}{2}\left(\frac{\nu_c}{\omega}\right)\left(\frac{\omega}{c}\right)\frac{\left(\frac{\omega_p}{\omega}\right)^2}{\left[\left(\frac{\nu_c}{\omega}\right)^4 - \left(\frac{\omega_p}{\omega}\right)^2\left(\frac{\nu_c}{\omega}\right)^2 + 1 + 2\left(\frac{\nu_c}{\omega}\right)^2 - \left(\frac{\omega_p}{\omega}\right)^2\right]^{\frac{1}{2}}}$$

Neglecting the first two terms in the denominator

$$\beta \simeq \frac{\frac{1}{2}\left(\frac{\nu_c}{\omega}\right)\left(\frac{\omega}{c}\right)\left(\frac{\omega_p}{\omega}\right)^2}{\left[1 + 2\left(\frac{\nu_c}{\omega}\right)^2 - \left(\frac{\omega_p}{\omega}\right)^2\right]^{\frac{1}{2}}}$$

Attenuation of the microwaves, collision frequency versus Mach number for various p_1 are plotted in figures (13-17).

Reference (27) gives plots of total attenuation per unit path length of gas $e^{-\beta\frac{v_0}{\omega}}$ and measurable phase shift $\left(1-\frac{\omega}{v_0\alpha}\right)e^{-\beta\frac{v_0}{\omega}}$ (α and β in units of $\frac{\omega}{v_0} = k_0$, v_0 - phase velocity in lossless dielectric) versus $\frac{\omega_p}{\omega}$, for several values of the collision parameter $\frac{\nu_c}{\omega}$ from 0 to 10. In the idealized case of zero collisions the value $w_p = w$ sharply divides the behavior of the medium into two distinct regimes, one dielectric, $w < w_p$, where the wave propagates without attenuation, and the other reactive, $w > w_p$, where the wave becomes evanescent. The effect of collision tends to smooth out the transition between these two regimes. For further discussion see the above mentioned report.[10]

(b) Collision Frequency for Argon

The collision frequency is given by $\nu_c = \frac{v_e}{l}$

l, is the mean free path of electrons between momentum transfer collisions (elastic) with argon atoms

v_e, is taken to be the equilibrium r.m.s. velocity of the electron = $\sqrt{\frac{3kT_e}{m_e}}$

This is an approximation.

The mean free path (Appendix) may be related inversely to the number density of the gas molecules N, and the collision cross-section of a gas molecule A. Thus the collision frequency is given by

$$l = \frac{1}{NA}$$

$$\nu_c = v_e NA \qquad N = \frac{\rho N_0}{M} = \frac{\rho N_0}{RT}$$

$$v_e = \sqrt{\frac{3k}{m_e}}\ \frac{A\rho N_0}{RT}\sqrt{T_e}$$

for $T = T_e$ temperature of the gas

$$\frac{\nu_c}{\omega} = \frac{4.28 \times 10^3 pA}{\sqrt{T}}$$

p - mm Hg
A - cm^2
T - °K

$w = 1.53 \times 10^{11}$ radians/sec

The collision cross-section for argon was obtained from a literature survey of experimental values.[11-23] There is, however, a lack of values in the region of low electron energy (.5ev or 5800°K). The data collected from the many experiments (fig. 11,12) show fairly large disagreement, values differing by a factor of about six. These curves show the anomalous Ramsauer effect (Appendix). Unfortunately our experimental conditions are in the regions where the cross-section is at a minimum.

These measurements were obtained principally by two methods:

(i) Direct: This scheme was first assembled by Ramsauer. His apparatus was built so that he could measure the intensity of the electron-beam as a function only of electron velocity. The electrons, accelerated from a source to a given velocity, were passed into a velocity filtering system consisting of several slits to collimate the beam. Measuring the electron current at one point and later at another point, the cross-section was then obtained, $I = I_o e^{-\alpha x}$. The accuracy of this type of measurement depended greatly on the width of the slit.

(ii) Indirect: This method was first used by Townsend. The drift velocity W, of electrons moving through a gas under the action of a uniform electric field was related to the field intensity $\mathcal{E}$, root mean square velocity u and the mean free path l

$$W = \frac{c\mathcal{E}el}{mu}$$

c - numerical factor which depends on the velocity distribution.

The values of collision cross-section which were used in the calculations to compute the attenuation of the microwaves are specified on the plots.

(c) Propagation of electromagnetic waves through a slab of ionized gas [24]

In the experiment the ionized gas is confined between the walls of the shock tube and is isolated from the microwave apparatus. The electromagnetic waves crossing the interfaces between the ionized gas and the walls are subject to reflection losses and phase changes. The transmitted waves must traverse two interfaces plus the

ionized medium*; the reflected waves will be influenced by reflections from the two interfaces and the intervening ionized gas, thus establishing the phase and amplitude of both signals. The incident waves are considered to be plane-polarized, transverse, harmonic time dependent. The assumption of the existence of similar reflected and transmitted waves, and positive and negative propagating waves within the ionized medium is made.

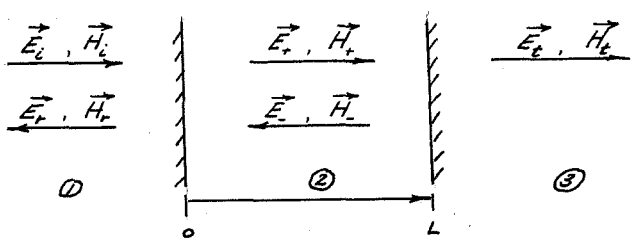

Assuming $\mu_1 = \mu_2 = \mu_3$ (permeability) and $k_1 = k_3$ (same media) the reflection and transmission coefficients become: (k^* - complex propagation constant)

$$R = \frac{E_1^-}{E_1^+} = \frac{\left(\frac{k_3}{k_2^*} - \frac{k_2^*}{k_1}\right)e^{ik_2^*L} + \left(\frac{k_2^*}{k_1} - \frac{k_3}{k_2^*}\right)e^{-ik_2^*L}}{\left(2 + \frac{k_3}{k_2^*} + \frac{k_2^*}{k_1}\right)e^{ik_2^*L} + \left(2 - \frac{k_3}{k_2^*} - \frac{k_2^*}{k_1}\right)e^{-ik_2^*L}}$$

$$\tau = \frac{E_3^+}{E_1^+} = \frac{4e^{ik_3L}}{\left(2 + \frac{k_2^*}{k_1} + \frac{k_3}{k_2^*}\right)e^{ik_2^*L} + \left(2 - \frac{k_3}{k_2^*} - \frac{k_2^*}{k_1}\right)e^{-ik_2^*L}}$$

---

* Note, this is a simplification of the actual problem. The electromagnetic waves, in addition to passing through two interfaces and the ionized medium, must traverse the dielectric windows of the horns, However, the windows have been made to be transparent to the microwaves. (see Section V.)

V. EXPERIMENTAL APPARATUS AND PROCEDURE

Shock Tube Facility and Instrumentations

An 8.2 centimeter square shock tube of commercial cold rolled steel with 1.59 centimeter thick walls and 360 centimeter in length was used in this experiment. The high pressure chamber also of the same material was circular in cross-section, 11.4 centimeter in diameter, and was 18.8 centimeter in length. Circular flanges with O ring grooves were welded to the mating ends of the two sections. The diaphragms were held in position by dowel pins and O rings, and the two ends connected together by a threaded sleeve. Ports on the sides of the tube were provided for film heat gauges to measure shock velocities and for the microwave horns.

The gas manifold system (fig.19) in the low pressure end of the tube was designed to handle the test gas and evaculation of the chamber. Circle seal plug valves were used throughout the system.

The vacuum pumping system consisted of a Consolidated Vacuum Corporation MCF-60 oil diffusion pump, using Dow Corning 703 Silicone oil, backed by a Kinney KC-8 double stage mechanical pump.

The leak rate for the tube was determined to be

about 1-5 μ per minute. This was primarily due to leakage at the ports where the heat gauge plugs and microwave horns were inserted. The vacuum sealing was accomplished by a sliding circular "O" ring which sat in a groove on the plugs and horns. We found this type of seal for high vacuum to be highly unsatisfactory but it could not be changed. A flow system was designed for removal of the residue gases and the reduction of impurities in the tube.

The pressure of the chamber at very low values was measured by a Consolidated Vacuum Corporation Phillip Gauge PH6-69; the test gas pressure for the experimental run was measured by a Wallace and Tiernan dial gauge (least reading 0.1 mm Hg). The uncertainty in measuring p_1 is about two percent.

The diaphragms used were DuPont mylar of thickness .001 to .01 inches. Several layers of mylar were used to obtain the desired thickness and strength to acquire the pressure ratio at which the diaphragms could burst by themselves. Shock velocities at similar conditions were reproduced to within one percent.

The thin platinum heat gauges, designed by Rabinowitz[33] were employed to measure shock velocities. The heat gauges were stationed either 67.7 cm or 10 cm apart. The voltage output of these gauges were fed into a Technology Instru-

mentation Company Type 500 A, 1000 gain wide band amplifier which in turn was connected to the Berkeley Model 7362 counter (least count of 1 μs). The first heat gauge served to trigger both the counter and oscilloscope simultaneously. A transitorized trigger amplifier was used to give a sharp spike to the input signal from the heat gauge to the oscilloscope in order to obtain consistency and accuracy in triggering. Setting the oscilloscope to trigger at 5 volts, the sweep was not delayed more than 1 μs. With the average transit time of the shock wave across the face of a heat gauge $\frac{1}{2}$ μs, the uncertainty in the measured shock velocity is about two and one-half percent.

The following procedure was established for setting up the shock tube.

(i) Clean tube of diaphragm fragments.

(ii) Seal tube with correct diaphragm.

(iii) Evacuate and flush with argon the low pressure section.

(iv) Evacuate the tube to .3 μ Hg.

(v) Set the flow system to give required initial conditions (p_1) (.03 gms/min.)

(vi) Tune the microwave (see next section).

(vii) Pressurize the compression chamber to required p_4 - 100 psi.

(viii) Retune the microwave.

(ix) Isolate the pressure gauges and shut off the flow.

(x) Set oscilloscope, camera, and counter.

(xi) Fire tube.

Microwave Instrumentation [28,29]

At the present time microwaves are the highest radio frequencies employed for communication, detection, control and navigation. The frequency range is approximately from .3 to 300 KMC with corresponding wavelengths from 100 to .1cm. An important application with regard to our experiment is the ability to concentrate the radiation within cones of a few degrees in width and to operate at high gain. This can be done only if the effective aperture of the antenna is many wavelengths wide.

The microwave network* is shown in fig (18). Each component is designed to minimize reflection losses. The following is a description of the components.

Rectangular waveguides (24 KMC, K-band) were used. The mode being propagated is the dominate H-mode. The klystron, a 2K50, 23.5 to 34.5 KMC, 10mw, 300V reflex type tube (Bendix Aviation Corp.) was used as the generator

---

* All components except the klystron and isolator were obtained from Demornay Bonardi Co.

of electromagnetic waves. The adapation of the power supply (Dessen and Barne #62-109) to the operation of the klystron is shown on fig. (20). An unfortunate feature of the circuitry was that the repeller voltage was coupled to the tuner grid voltage of the klystron. The repeller voltage was adjusted in tuning of the microwave apparatus to obtain the mode where the klystron would generate peak power to minimize the effect of line fluctuations. Since the klystron was thermally tuned a fan was used to maintain it at a constant temperature. The detector consist of a crystal, silicon, coaxial type diode (IN26), and a tunable crystal mount to match the reactive component of the crystal impedance. The time constant of the unit was less than a microsecond. The power response of the crystals obeyed the square law in regions below 15 microwatts; above this the crystals were required to be calibrated which they were in this experiment. The E-H plane tuner was used as a matching transformer to correct mismatch between the klystron and the waveguide system. Isolation between the klystron and energy reflected from line mismatches (21.2 db, 24KMC) to insure maximum power and constant frequency output was furnished by a Uniline ferrite 25w load isolator, model K-131. The frequency was measured by a cavity meter to within .01KMC.

Two conical horns were constructed to fit tightly into the ports of the shock tube such that the base would be flush with the walls of the tube. A transformation of the H_{10} -mode travelling in the rectangular guide to the H_{11} - mode in the circular guide of the horn was made. The base of the horn is 1.3 inches in diameter and 11.5 inches in length. For purposes of input and output impedance matching (simulating $\frac{1}{4}$ wavelength plate for complete transmission), rexolite dielectric cones were secured to the exit glass windows of the horns. The horns, as a result, gave standing wave ratio of 1.24 and 1.25.

The component of the magnetic field vector in the direction of propagation in travelling through the conical horn will vary as $\frac{1}{r^2}$ with distance from the entrance of the horn. In the far zone region of the horn (where $kr >> 1$, k-propagation constant) the radial components of the field are negligibly small in comparison to the transverse components, and the field is predominately a transverse spherical wave which will become plane a few wavelengths outside of the horn.

The radiation pattern of the horn over the width of the shock tube must be considered to be the near zone pattern. Although no focusing of the beam was attempted by lenses, the horns, aperture of 3.3 wavelengths, were designed to produce a directive pencil beam. Knowledge of the

beam width and whether there were large side lobes was very important in the interpretation of our data. Several crude attempts were made to measure the width of the beam.

(a) using a copper plate and moving it perpendicular to the beam.

(b) filling a tube section standing on end until the water level reached the beam.

(c) placing the transmitting horn at a stationary position and moving the receiving horn in a circular arc at different radial distances to trace out the radiation pattern.

In instances (a) and (b) the width of the beam was found to be smaller than the aperture of the horn and from (c) no large side lobes were evident.

Another important point in the radiation pattern is whether the reflections from the upper and lower walls are small. The height from the edge of the horn to the walls was found to be 3.45 wavelengths. For any appreciable reflection to reach the receiving horn or to interfere with the incident beam, radiation must predominately come from waves directed at an angle of 40 degrees or more relative to the center lines between horns. Since the measured pattern showed no prominent side lobes, we considered this problem as being minor.

Two signals, transmission through and reflection from the ionized gas measured by detectors (A) and (B) respectively, must be uncoupled, i.e. any reflection should have negligible effect on the transmission and should not untune the microwave network. We could check this by causing reflection from terminator (A) (adjusting the stub tuner) to show up as a first order change in the reflected signal (increase) at the detector (B) and a second order change (decrease) in the transmitted signal at detector (A) Reflection from detector (A) (mismatching the detector) should cause changes of the same order in the two signals. The uncoupling was effected by the magic tee in that if the load impedance of the two collinear arms were equal, the signal fed into the shunt arm would be divided equally between the two collinear arms. Because of the symmetry of the structure, there would be no coupling between the series and shunt arms. As there was no net electric vector developed across the entrance to the series arm. Similar symmetry conditions existed for signals being propagated along one collinear arm to be divided between shunt and series arm of magic tee.

For maximum sensitivity and stability of the microwave signal the amplifiers of the oscilloscope were usually set at 50 mv/cm for the transmitted signal and at 20mv/cm for the smaller reflected signal. To obtain maximum var-

iation of the signal (.55V) on the oscilloscope face the input signal was attenuated. The system had to be retuned after the diaphragms were stressed close to bursting pressure. This was because the metallic shock tube acted like a resonating cavity for the power radiated away and not received by the horn; a standing wave pattern was established in the tube. It was observed that by stressing the diaphragm the length of the cavity was essentially changed which in turn altered the power transmitted across the tube.

The tuning condition required maximum transmission and minimum reflection of the signal at the condition (p_1) before the tube was fired. Hence any increase or decrease of the signal during the experiment can be attributed only to the passage of the shock. The procedure for tuning was as follows:-

(a) Set beam voltage to +300 VDC, tuner grid voltage to about -9VDC.

(b) Adjust the repeller voltage for maximum power output by observing the transmitted signal (voltage) at detector (A).

(c) Adjust crystal mount to match impedence of crystal. Tune crystal diode to give maximum reception (minimum reflection).

(d) Adjust the E-H plane tuner to correct mismatch between the klystron and the waveguide system.

(e) Replace the terminator (B) by detector (B) and adjust for peak reception.

(f) Repeat (c).

(g) Tune out reflections from the glass-gas interface (see fig. 18) and signal from klystron using the variable stub tuner.

(h) Repeat (c).

(i) Set amplifiers of the oscilloscope at the desired sensitivity for the transmitted signal and reflected signal.

(j) Attenuate transmitted signal for maximum variation on the scope face. Repeat (c) and (g)

(k) Repeat (c) and (g) after the shock tube diaphragm is stressed (p_4 - 100 psi)

VI. RESULTS AND DISCUSSION

In the experiment of the attenuation of electromagnetic waves by electrons there are essentially two unknowns, the collision cross-section and the electron density. In section IV the measurements of collision cross-sections by previous investigators in our energy range show large disagreement. A recent calculation by Kivel[22] shows that his curve is best fitted by the measurements of Ramsauer and Kolloth. The calculations of electron density by the shock tube relations and the Saha equation, derived from statistical mechanics, are better understood and are on firmer grounds than the theory for collision cross-section. However, the experiment may not exactly conform to the assumptions made in the theory and the errors thus introduced could possibly set the two unknowns on the same footing.

The testswere run at $p_1 = 5$mm and 10mm. The Mach number ranged from 6.19 to 7.74 with corresponding computed electron density as large as $1.6 \times 10^{13}/_{cm^3}$. Typical responses of the microwave to the passage of the incident shock are shown in figure (24). On these records the downward deflection of the upper trace corresponded to a lower intensity of signal reaching the detector, i.e. the transmitted signal was increasingly attenuated until equilibrium was reached behind the shock (region (1) of the middle photograph). The

upward deflection of the lower trace corresponded to an increase in intensity of the reflected signal from the gas. Region (2) represented the point when equilibrium was reached behind the shock and where the signal was constant. Region (3) indicated the arrival of the cold front resulting in a decrease of the attenuation due to a decrease in electron concentration.

The overall microwave attenuation across the test section could be divided into two parts - absorption loss and reflection loss. The present experiments indicated that the reflection loss was quite small compared with the absorption loss, even when the collision frequency ν_c was relatively small compared to the plasma frequency W_p. The measured values of attenuation were compared with the theoretical curves based on thermal equilibrium conditions behind the normal shocks (figures 15,16). The observed microwave attenuation at the lower shock speeds fell consistently below the predicted values by a considerable amount. This fact seemed to indicate either that the collision cross-section used in the calculations was too small or that the electron density was too low, probably the former. However, the reflected signals should provide additional information on this point, but because of the inconsistency and unreliability of these measurements no conclusions were reached.

The ionization relaxation time of argon (figs. 21,22, 23) was seen to decrease with increasing Mach numbers, thus

corresponding to an increase in the temperature and a slight increase in the density. For runs at the same Mach numbers but at a sizeable increase in density there was a decided decrease in the relaxation time. The microwave apparatus was insensitive to electron level below 9×10^{10}. With this sensitivity there was no indication that there was ionization of a greater degree than this ahead of the shock.[1] The microwaves traces did not begin to deflect until 20 to 50 after the shock had passed the horns. No theory had been developed here for the rate of ionization, but the results were compared with the extrapolation of the theory by Petschek[1], which does not really apply to our experimental conditions because of a significant difference in electron concentration. The data on the influence of impurities on the rate of ionization was not conclusive. Based on rough calculations using the Gilmore tables[36] the contribution of electrons from impurities (air) in the bottled argon (commercial grade Linde's) at a temperature about 5000°K ($M = 7$, $p_1 = 5$mm, $n_e = 1.7 \times 10^{11}$ electrons/$_{cm^3}$ from pure argon) was estimated to be 9×10^{8} electrons/$_{cm^3}$. For a leak rate of 10μ /min. of air, the electron contribution was about 2.4×10^{10} electrons/$_{cm^3}$. There was no significant change on the relaxation using the flow system (.03gm/min.) after the tube was pumped to .3μ compared to the case when the shock tube was evacuated to .1μ with no flow system. No refined method for introducing controlled amount of impurity was attempted.

Experimental difficulties.

On several of the records the beginning of the traces were displaced from their original settings. This indicated that the microwave circuit was mistuned at the time the diaphragm ruptured. As a result the traces often were deflected in the wrong direction and these records were disregarded. The traces shown (fig. 24) should presumably be smooth curves, but a superimposed low frequency wave ($\sim 2 \times 10^4$ cps) can be seen on them. Calculations tended to indicate this to be the Doppler effect. The microwaves which were scattered were reflected from the moving shock front. The frequency of the reflected waves was either increased or decreased depending upon whether the shock was ahead or behind the horns; the phase velocity depended upon whether the waves travelled through neutral or ionized argon. As a result of this the reflected signals interacted with the signals which were being transmitted across the shock tube, thus setting up an interference pattern. The interference pattern caused some difficulty in the determination of the level of equilibrium and the time when equilibrium was reached. (A probable remedy would be to make the test section and the tube ends of some absorbent material)

Theortically, the reflected signal from the gas was expected to increase and then come to some equilibrium value (similar to transmitted signal) after the shock passed. The

experimental results showed that this was not always true. The reflection became largest during the non-equilibrium period and was decreasing when equilibrium was reached in the transmitted signal. Possible mistuning, unknown electron distribution in region of the wall and the Doppler effect added complications to the interpretation of the data.

After the passage of the cold front the traces should return to their original values as the electron density became negligible. The reflected signal did return, but the transmitted signal levelled off at some intermediate value. To investigate this tests were made to check the effect of density changes (other than ionization) on the dielectric. To show that the density effect could be separated from the ionizing effect we ran tests at low Mach numbers where ionization was negligible, but with the same density condition as behind shocks at the larger Mach numbers. These tests showed that the transmitted signal was attenuated only after the cold front had passed. When the cold front was not well defined, the signal did not change as abruptly as expected. Static tests were also made where the microwave equipment was tuned at p_1 and the tube pressure was then increased at intervals. Similar reaction of the signal was seen, where the signal did not change greatly until the density condition was close to that in the experiment. The calculations of the influence of the dielectric change due

to density, using the approximate Clausius and Mossotti relation[32,35], ($\frac{n-1}{\rho}$ = constant, n = refractive index) in the wavelength was found to be negligible ($\frac{\lambda_1}{\lambda_0} = \frac{n_1}{n_0} = .99948$ $n_0 - 1 = 277.8 \times 10^{-6}$, $p_o = 760$mm) based on conditions which existed behind the cold front in helium. This small change in the wavelength over the length or width of the tube did not account for the apparent change in the amplitude of the signal. However this portion of the trace was unimportant in obtaining the required data unless this drop in the signal level occurred during the testing time.

VII. CONCLUSION

The preliminary experiments on the microwave probing of ionized argon described in this paper have demonstrated the ultility of the technique and presented results which agree qualitatively with theoretical predictions. They have also demonstrated the complexity of the interactions involved and emphasized the need for more refinement in the apparatus and technique and better control of the experimental conditions if reliable quantitative data is to be obtained.

REFERENCES

1. Petschek, H. E., Approach to Equilibrium Ionization Behind Strong Shock Waves in Argon, Ph. D. Thesis, Graduate School of Aeronautical Engineering, Cornell University.

2. Lin, S. C., Avco Research Laboratory, Research Report.

3. Wray, K., Teare, J.D., Kivel, B., and Hammerling, P. Avco Research Laboratory, Research Report 83.

4. Lin, S. C., Avco Research Laboratory, Research Report 33.

5. Turner, E. B., The Production of Very High Temperature in the Shock Tube with an Application to the Study of Spectral Line Broadening, ASTIA., AD 86309.

6. Fowler and Guggenheim, Statistical Thermodynamics, Cambridge, The University Press, (1920).

7. Liepmann and Roshko, Elements of Gasdynamics, Wiley, (1957).

8. Lin, S. C., Kesler, E.L., and Kantrowitz, A.R., Jour. Appl. Phys. 26, 95 (1955)

9. Weymann, H. D., On the Mechanism of Thermal Ionization Behind Strong Shock Waves., University of Maryland (1958)

10. Whitmer, R. F., RADC, TR - 59 - 203

11. Ramsauer and Kolloth, Ann. der Physik
    4, 91-95 (1930)
    3, 536-539 (1929)
    64, 518-522 (1921)
    451-453 (1921)
    66, 546-549 (1921)
    12, 529-533 (1932)
    837-839 (1932)

REFERENCES

11. Ramsauer and Kolloth, (continued)
Phys. Zeits.
72, 345-349 (1923)
22, 867-870 (1931)
20, 823-826 (1928)
31, 985-989 (1930)
81, 1-3 (1928)

12. Normand, C. E., Phys. Rev. 35, 1217-1220 (1930)

13. Brode, R. B., Rev. Mod. Phys. 5, 257-260 (1932)
Phys. Rev. 25, 636-639 (1925)
35, 504-507 (1930)
37, 570-571 (1931)
34, 673-675 (1929)
Proc. Roy. Soc. CIX, 397-400 (1925)
CXXV, 134-137 (1929)

14. Rusch, M., Phys. Zeits. 26, 748-750 (1925)

15. Bruche, E., Ann. der Phys. 82, 912-915 (1927)
83, 1066-1069 (1927)
84, 279-282 (1927)
81, 537-539 (1926)
1, 93-94 (1929)
Phys. Ztschr. 29, 830-833 (1928)
26, 748-751 (1925)

16. Meyer, H. F., Ann. der Phys. 64, 451-454 (1921)
Phys. Rev. 64, 451-453 (1921)
468-469 (1921)

17. Townsend and Bailey,
Phil. Mag. 44, 1035-1038 (1922)
47, 379-381 (1924)
Proc. Roy. Soc. 120, 511-513 (1928)
88, 336-338 (1913)

18. Arnot, F. L., Proc. Roy. Soc. 133, 615-617 (1931)
Collision Processes in Gases,
Methaen's Monographs (1933)

19. Wahlen, N. B., Phy. Rev. 37, 262-265 (1931)

20. Meyer, H. F., Ann. der Phys. 64, 451-454 (1921)

21. Rose and Brown, Jour. of App. Phys. 23, 1028-1030 (1952)
Phys. Rev. 89, 559-561 (1951)

REFERENCES

22. Kivel, Avco Research Laboratory, Research Report.

23. Pack, J. L., Phys. Rev. Letters (Oct. 1959)

24. Stratton, J.S., Electromagnetic Theory, McGraw-Hill (1941)

25. Massey and Burlop, Electronic and Ionic Impact Phenomena, Oxford (1952)

26. Mott and Massey, The Theory of Atomic Collision, 2nd Edition, Oxford (1949)

27. Jahn, R., Interaction of Electromagnetic Waves with Slightly Ionized Gases, Guggenheim Jet Prop. Center Tech. Rep. (1960)

28. Borgnis, F. E. and Papas, C. H., Electromagnetic Waveguides and Resonators, Berlin, Springer, (1955)

29. Ginzton, E. L., Microwave Measurements, McGraw-Hill, (1959)

30. Albini, F. and Jahn, R., Reflection and Transmission of Electromagnetic Waves at Electron Density Gradients, Jour. App. Phys. to be published Guggenheim Jet Prop. Center Tech. Rep. (1960)

31. Margenau, H., Phys. Rev. 109, 6-9 (1958)

32. Lorentz, H. A., The Theory of Electrons, Dover Publication, (1952), p. 143

33. Rabinowitz, J., Jessey, M.E. and Bartsch, C.A., Appl. Phys. 27, 97-98 (1956)

34. Manheimer, Y., Timmat and Low, J. Fl. Mec. 6, 449 (1959)

35. Essen, Proc. Phys. Soc. B64, 862

36. Gilmore, F. R., Rand Corporation, RM-1543 (August 24, 1955)

VIII. APPENDIX

Concept of a Collision Cross-Section.[25,26]

A collision results when the relative distance between two particles is first decreased and then increased provided there is some physical change in either of the particles during the process. Thus if an atom is excited or ionized when an electron passes by it, or if the electron is deflected or has its energy altered, a collision has occurred.

From kinetic theory where the molecules and atoms are considered as solid spheres, a collision will occur whenever their centers approach each other with a distance, $r_{12} = r_1 + r_2$, sum of their radii. It can be shown from kinetic theory of gases that the mean-free-path l_1 of particles of type (1) moving amongst particles of type (2) is

$$l_1 = \frac{1}{\pi N_2 r_{12}^2 \left[1 + \frac{\bar{c}_2^2}{\bar{c}_1^2}\right]^{\frac{1}{2}}}$$

N_2 = number density of particles of type (2)

$\bar{c}_1, \bar{c}_2$ = root mean square velocities

If particles are of the same type

$$l = \frac{1}{\sqrt{2}\pi N d^2} \qquad r_{12} = 2r_1 = d$$

Let us consider the mean free path of an electron moving through the gas. In general its velocity will be much greater than the velocity of the gas molecules, thus the

mean free path becomes

$$l_0 = \frac{4}{\pi N d^2} = \frac{1}{NA}$$

$A = \frac{\pi}{4} d^2$, is the effective cross-section of the atom. Experimentally we can pass a beam of electrons of homogeneous velocity through a hypothetical gas consisting of solid spherical atoms of cross-sectional area, A. If there are N such atoms per cubic centimeter, the chance that an electron will make a collision in moving a small distance δx through the gas will be $NA\,\delta x$. Regarding any such impacts as moving an electron from the beam, the amount of the beam current strength lost in traversing a distance δx from a point will be

$$\delta I = NAI\,\delta x$$

$$I = I_0 e^{-NAx}$$

$$I = I_0 e^{-\alpha x}$$

$\alpha = NA$, is regarded as an absorption coefficient of the gas for the electron beam or the total (sum) effective cross-section in a cubic centimeter of gas.

We know that an atom really has no definite area of cross-section. The actual gas atoms are not rigid spheres with defined boundaries; the force between an electron and an atom will fall off continuously with distance and not

drop suddenly to zero at some definite separation. The beam loses current strength whenever an electron is deviated from its path or loses energy or both. Classically, as long as a field exists between an electron and atom, some deviation will occur. If this is true, then the effective cross-section of an atom will be infinite and the observed value is limited by the resolving power of the apparatus. If we turn to quantum mechanics for an explanation we do not have this dilemma. From the quantum uncertainty principle a definite value of the total effective cross-section is to be expected, provided the force between an atom and electron falls off at large separation faster than $\frac{1}{r^3}$ and a certain minimum resolving power is achieved. This means that deviations of a certain amount are not observed. Thus a collision cross-section of an atom is just a fictitious area and that if a particle passes through this area a collision will result. This imaginary area A is called the effective cross-section of the atom.

The question now arises; is the cross-section only a function of the geometrical configuration of the atom. As a consequence of the gradual decrease of the scattering field with distance as contrasted with the rigid sphere case, the total effective cross-section must be expected to vary with electron velocity. The variation of collision cross-section of rare gases with energy has been measured

experimentally by many investigators. Figures (11,12) show the variation of collision cross-section for elastic collision between argon and electrons. The straight line represents the kinetic theory value of the total effective cross-section. The measured values, however, show marked differences from those based on classical ideas. The slower the electrons the more effectively should they be scattered by the atomic field and hence the larger the cross-section. On the contrary a pronounced maximum is observed for electrons with energy in the neighborhood of 8 ev.; the gas is practically transparent to electrons about .6 ev, while for slower electrons the cross-section rises again. The fact that some atoms are effectively smaller obstacles to faster than slower electrons is known as the Ramsauer effect. This effect is by no means typical of other atoms.

The Ramsauer effect is somewhat analogous to the transmission resonances obtained in the one-dimensional potential well. In the case where the energy of the electrons is greater than the potential we would expect classically that all the waves would be transmitted. In quantum mechanics, however, some part of the wave is reflected at the sharp edges of the potential. If the waves reflect from the surfaces and interfere constructively with the oncoming waves the transmitted waves are reinforced. Thus for certain wavelengths the transmission coefficient is

unity. The analogy however, is not complete, because the condition for the Ramsauer effect is not exactly the same as that for a transmission resonance in a one-dimensional well. The reason for the difference is that in the one-dimensional case we define the transmitted waves as total waves that come through the well. In the scattering problem we have an incident wave that approaches on the well. Some of it enters the well and some of it is reflected at the edge of the well. The net effect is to produce an out-going wave, whose phase depends on what happens to the wave at the well. How much this outgoing wave corresponds to a scattered wave depends on how large a phase shift it has undergone relative to the out-going wave which is present in the absence of a potential. Thus we see that the intensity of the scattered and transmitted waves depends on somewhat different properties of the potential. The vanishing of the cross-section in the Ramsauer effect is a result of the fact that the contributions of different parts of the potential all add up in such a way as to produce a wave that cannot be distinguished from one which has not been inside a potential.

FIG. 1 PRESSURE RATIO VS MACH NO.

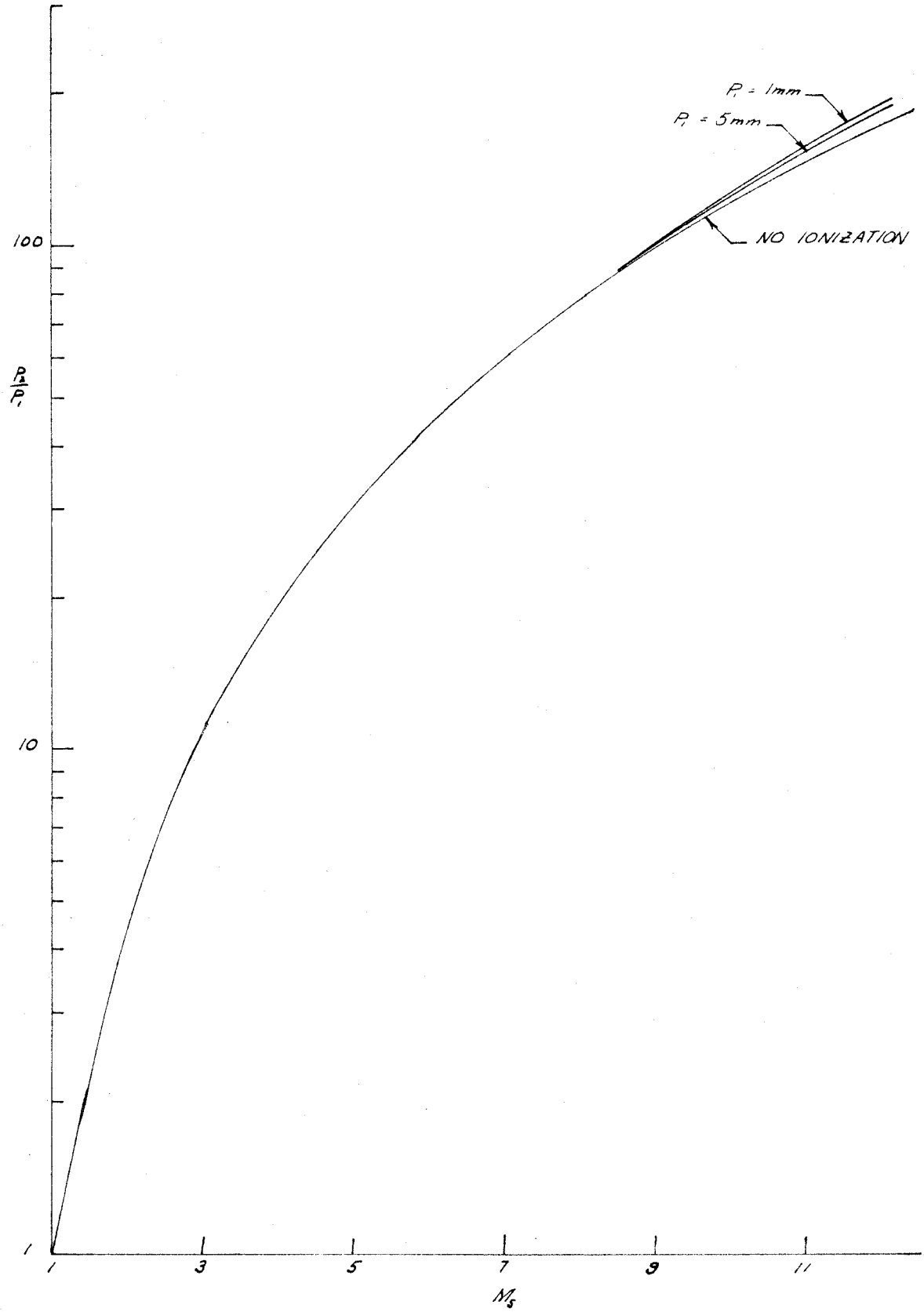

FIG. 2 DENSITY RATIO VS MACH NO.

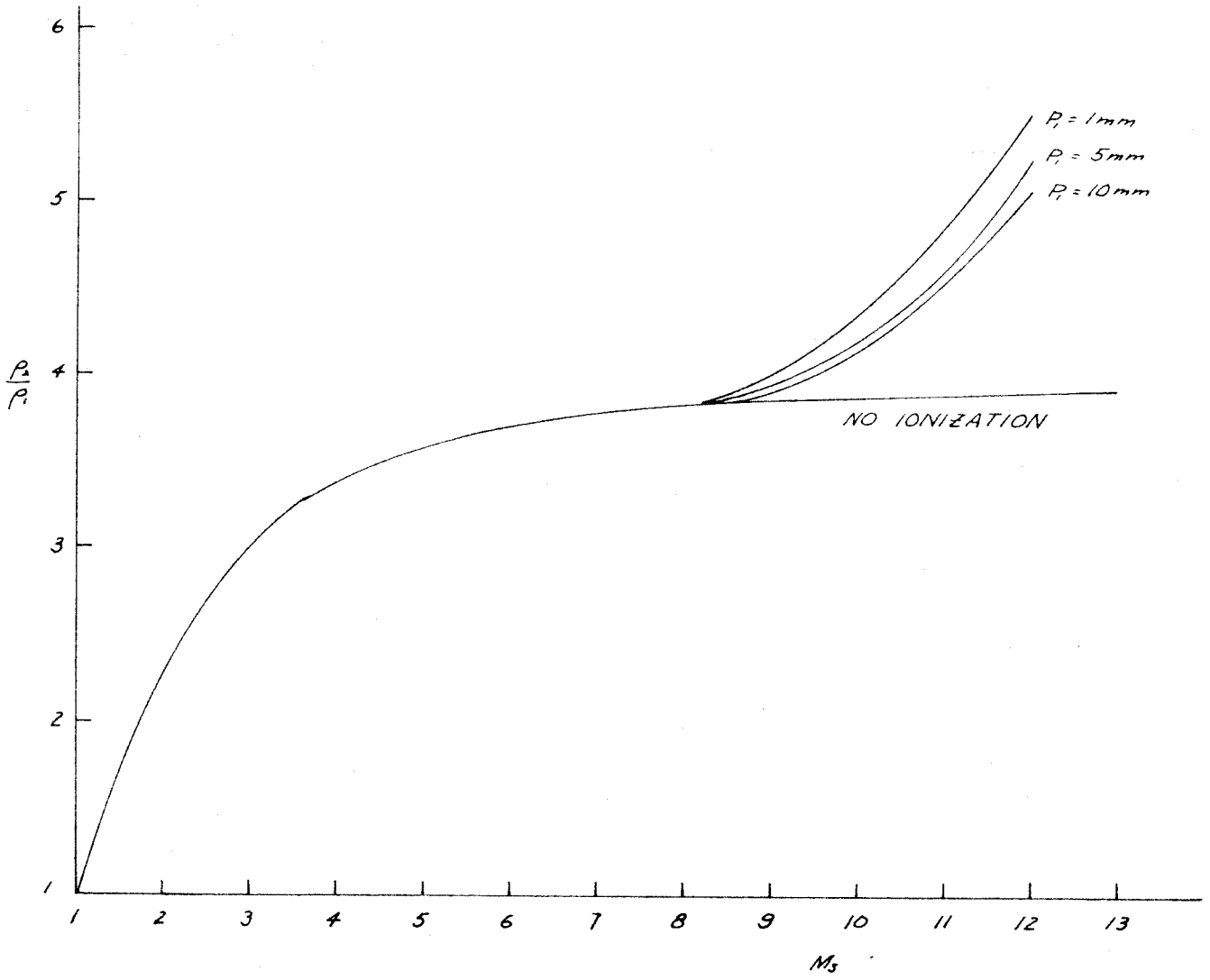

FIG 3 TEMPERATURE RATIO VS MACH NO.

$T_1 = 300\,^{\circ}K$

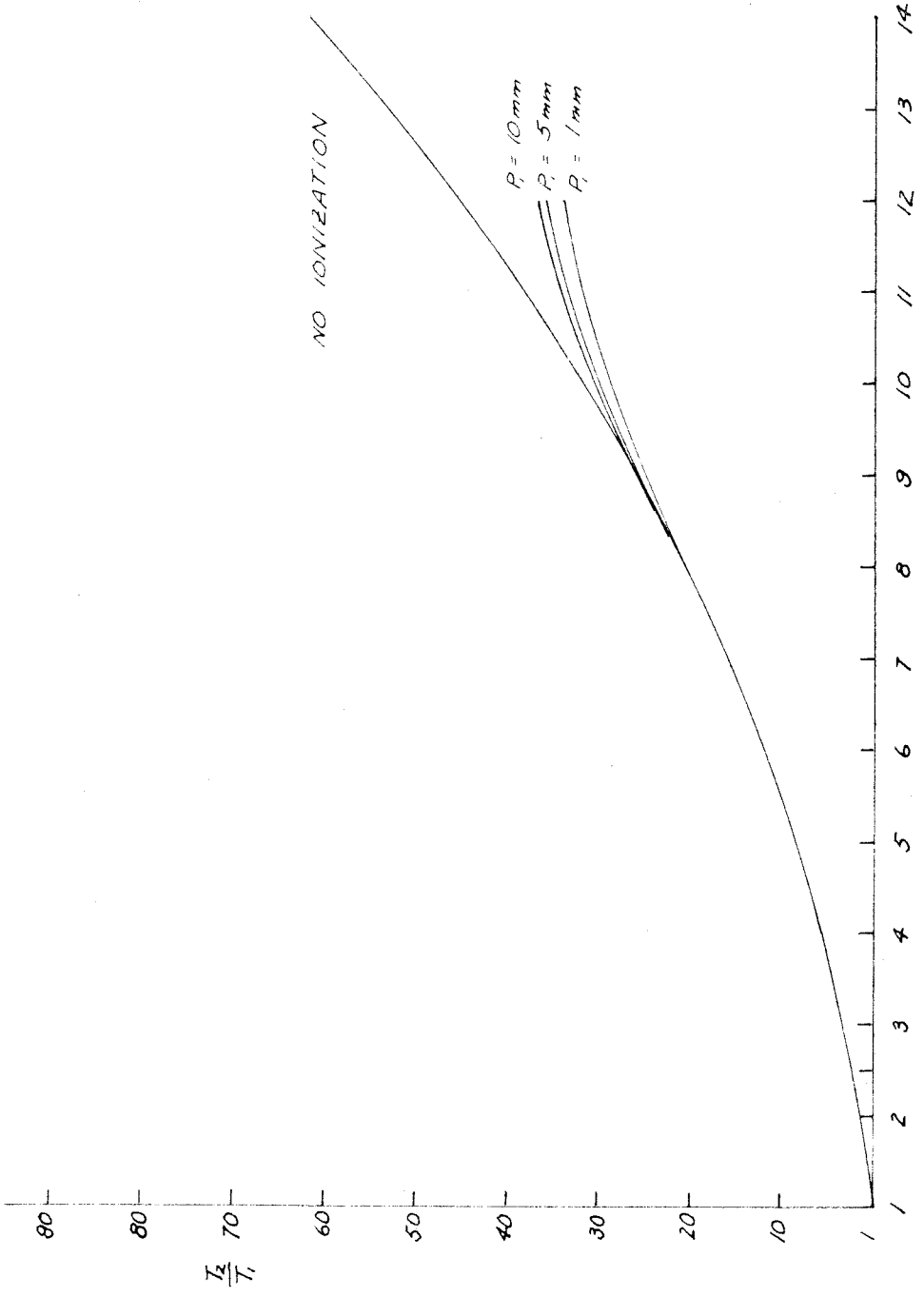

FIG. 4 DEGREE OF IONIZATION VS INCIDENT SHOCK

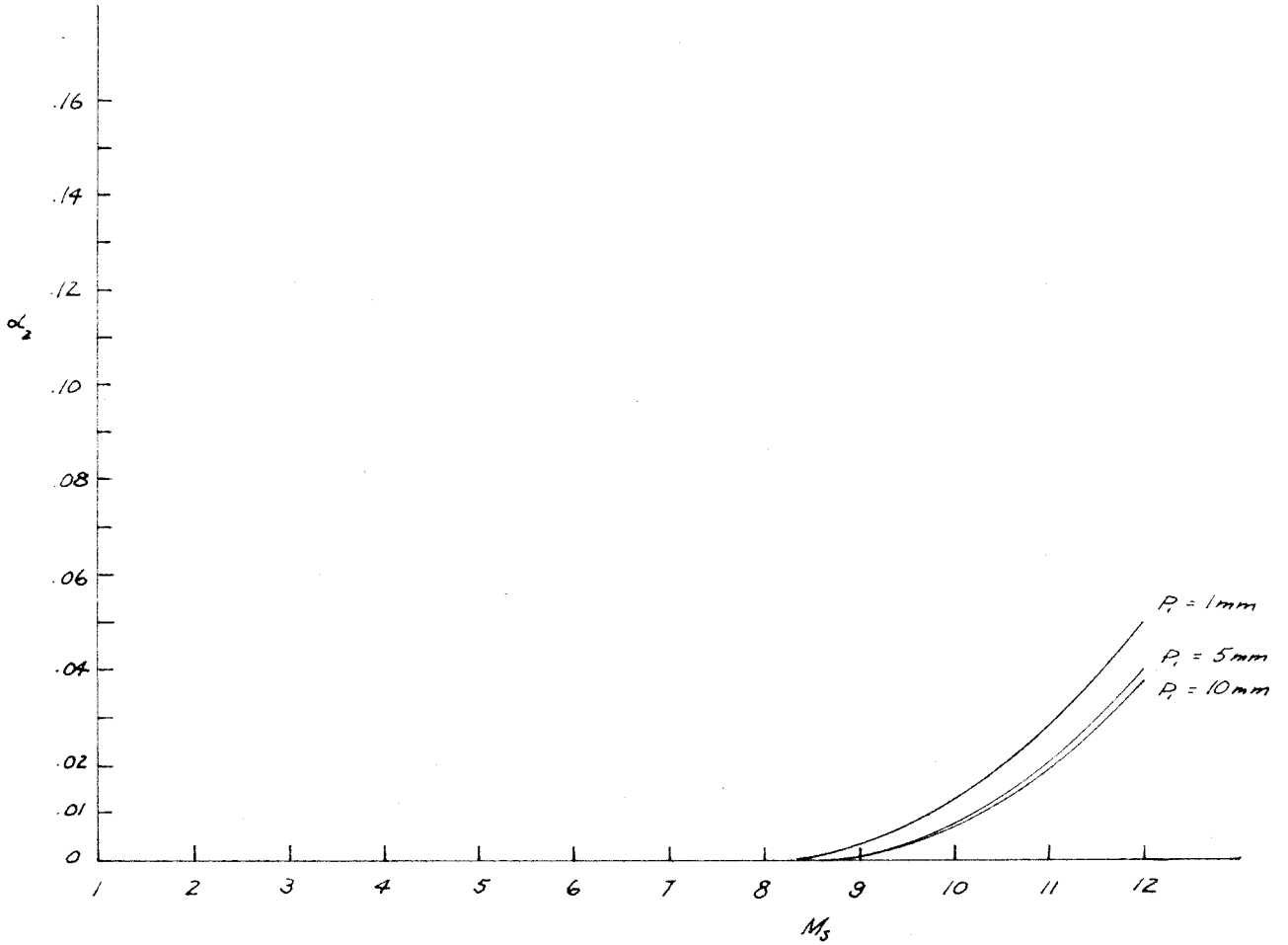

FIG. 5 COMPRESSION CHAMBER PRESSURE RATIO VS MACH NO.

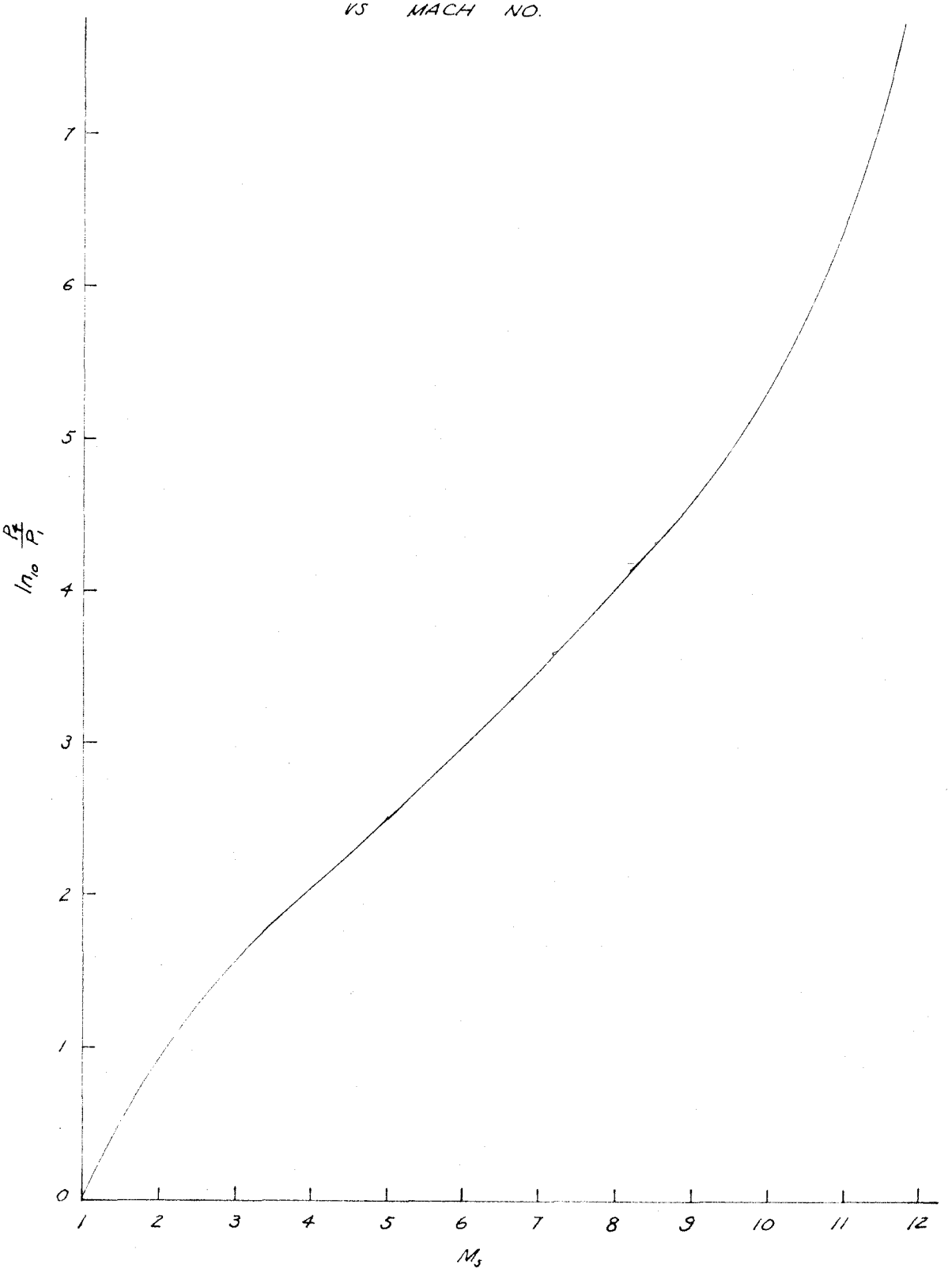

FIG. 6 PRESSURE RATIO VS MACH NO.

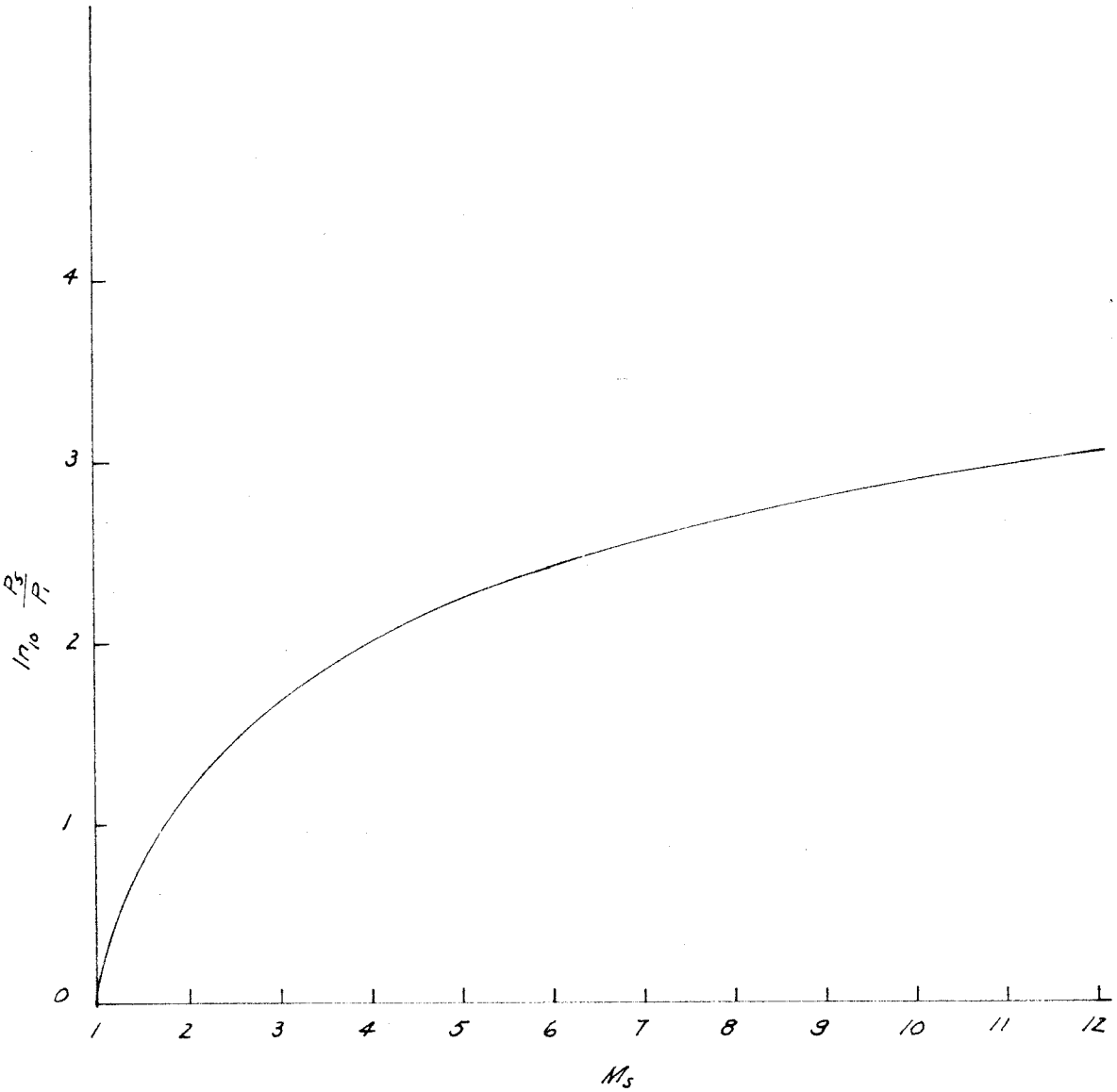

FIG. 7 TEMPERATURE RATIO VS MACH NO.

$T_1 = 300\ ^\circ K$

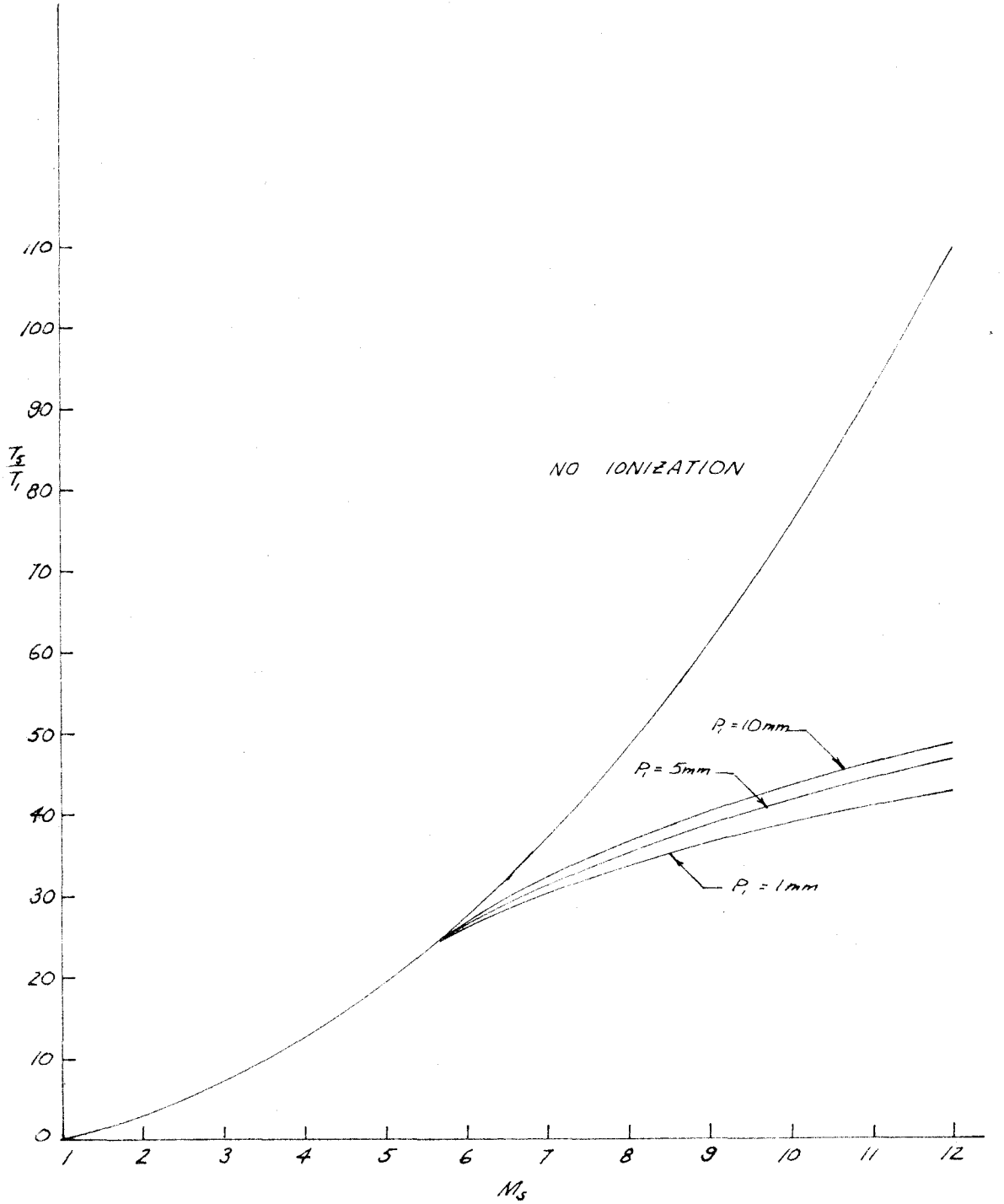

FIG. 8 DENSITY BEHIND REFLECTED SHOCK VS INCIDENT SHOCK

$T_1 = 300\ ^\circ K$

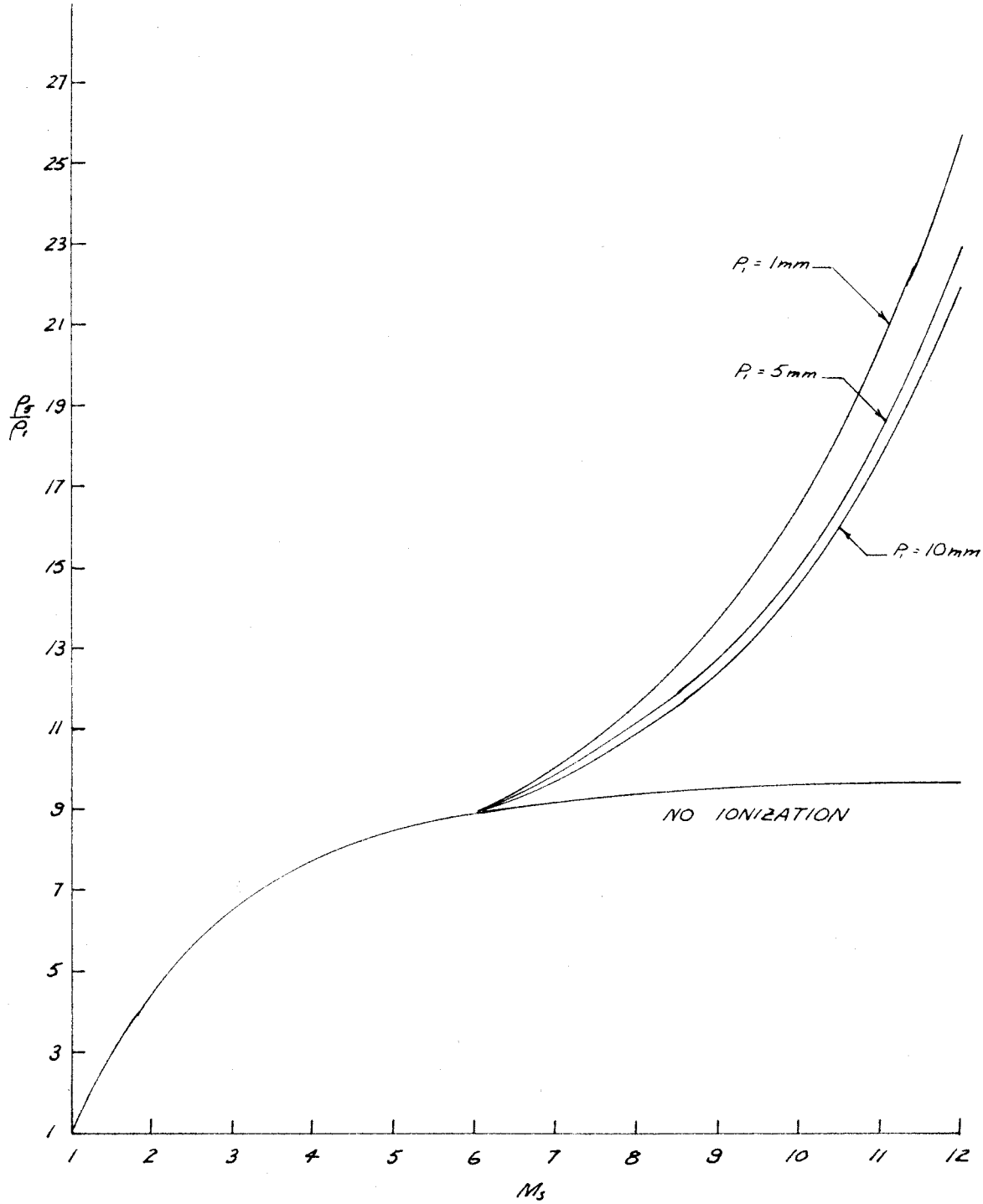

FIG. 9 DEGREE OF IONIZATION BEHIND REFLECTED SHOCK VS INCIDENT SHOCK

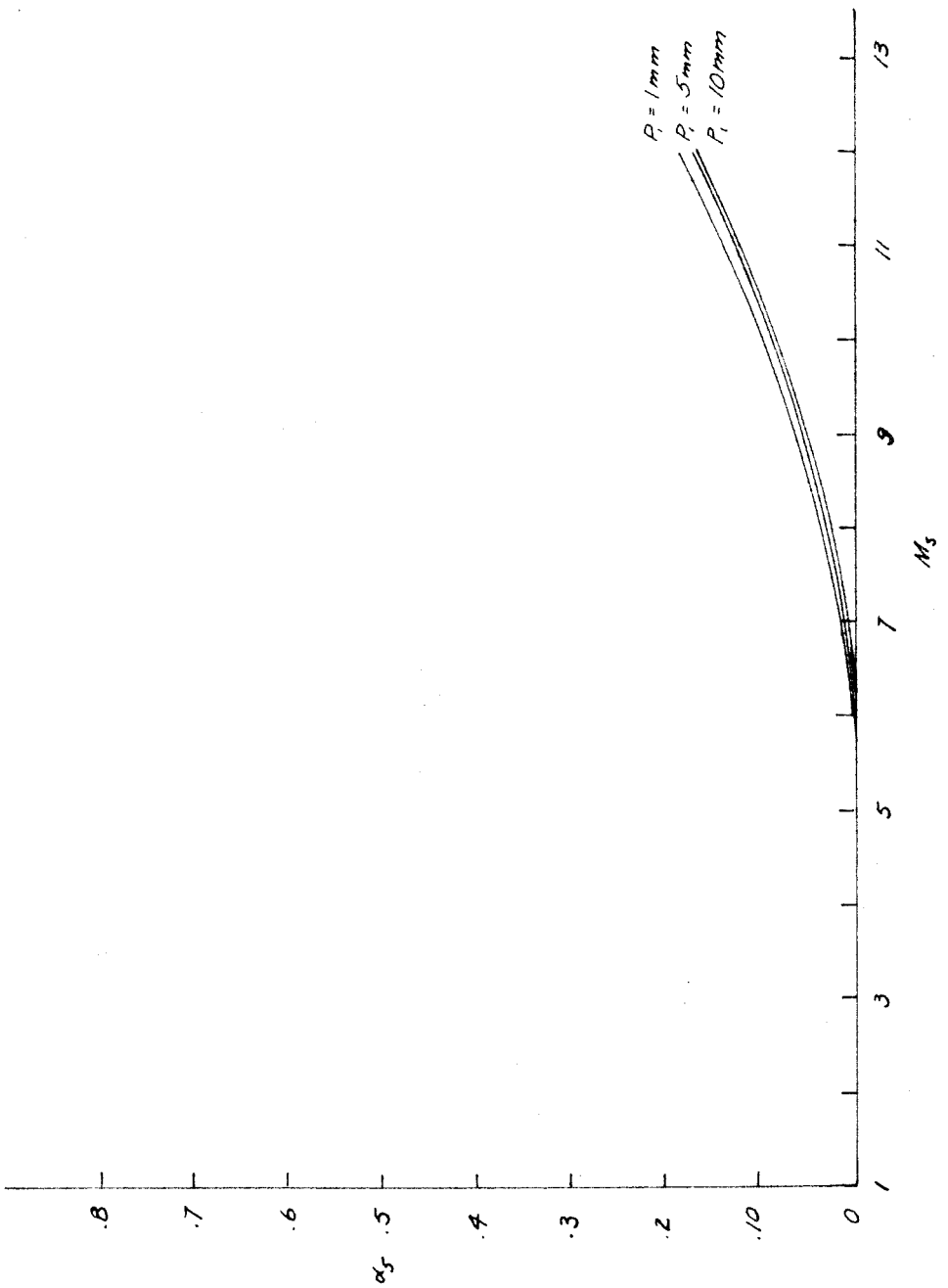

FIG. 10 ELECTRON DENSITY VS MACH NO.

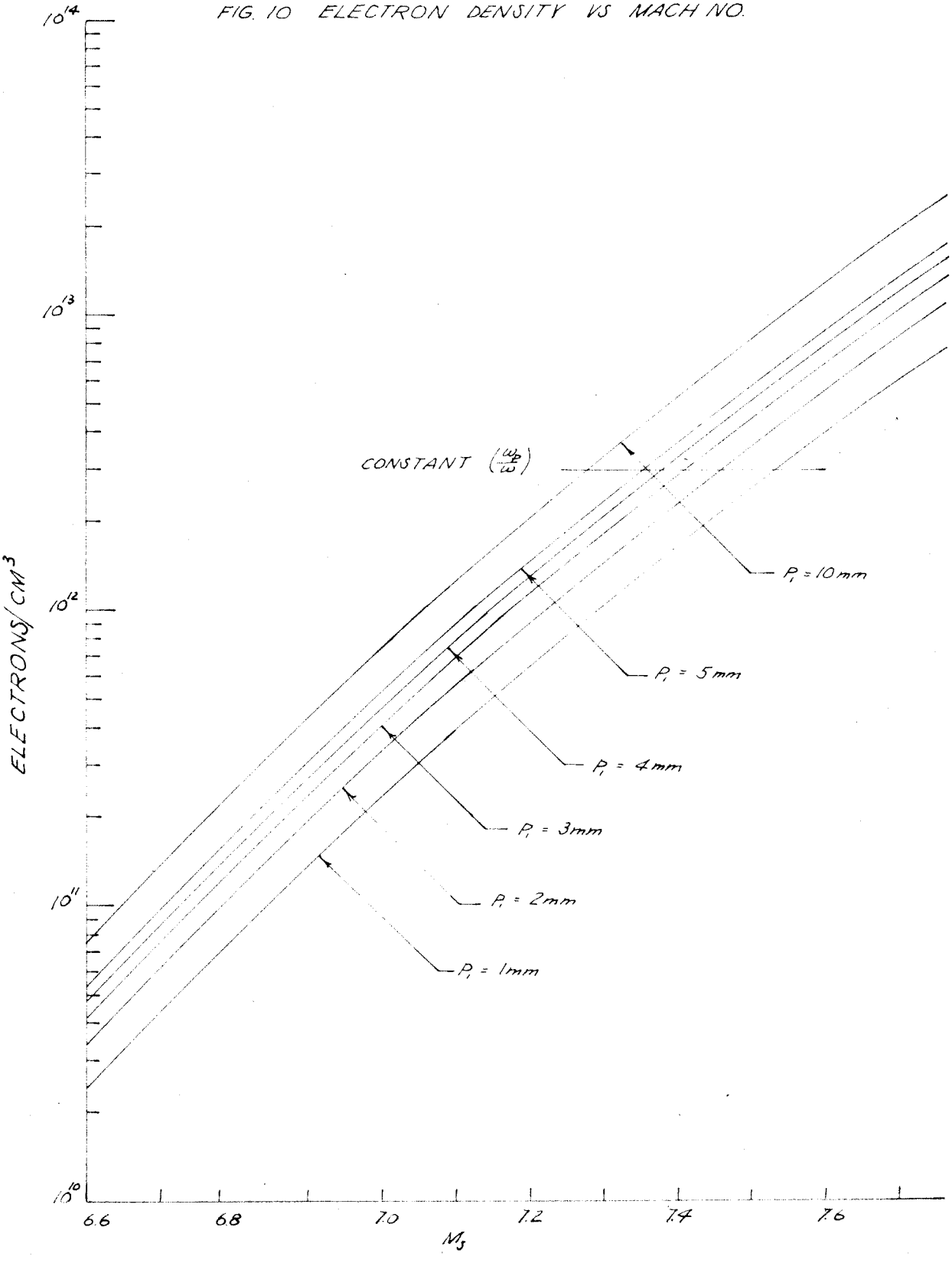

FIG. 11 COLLISION CROSS-SECTION OF ARGON VS ELECTRON ENERGY

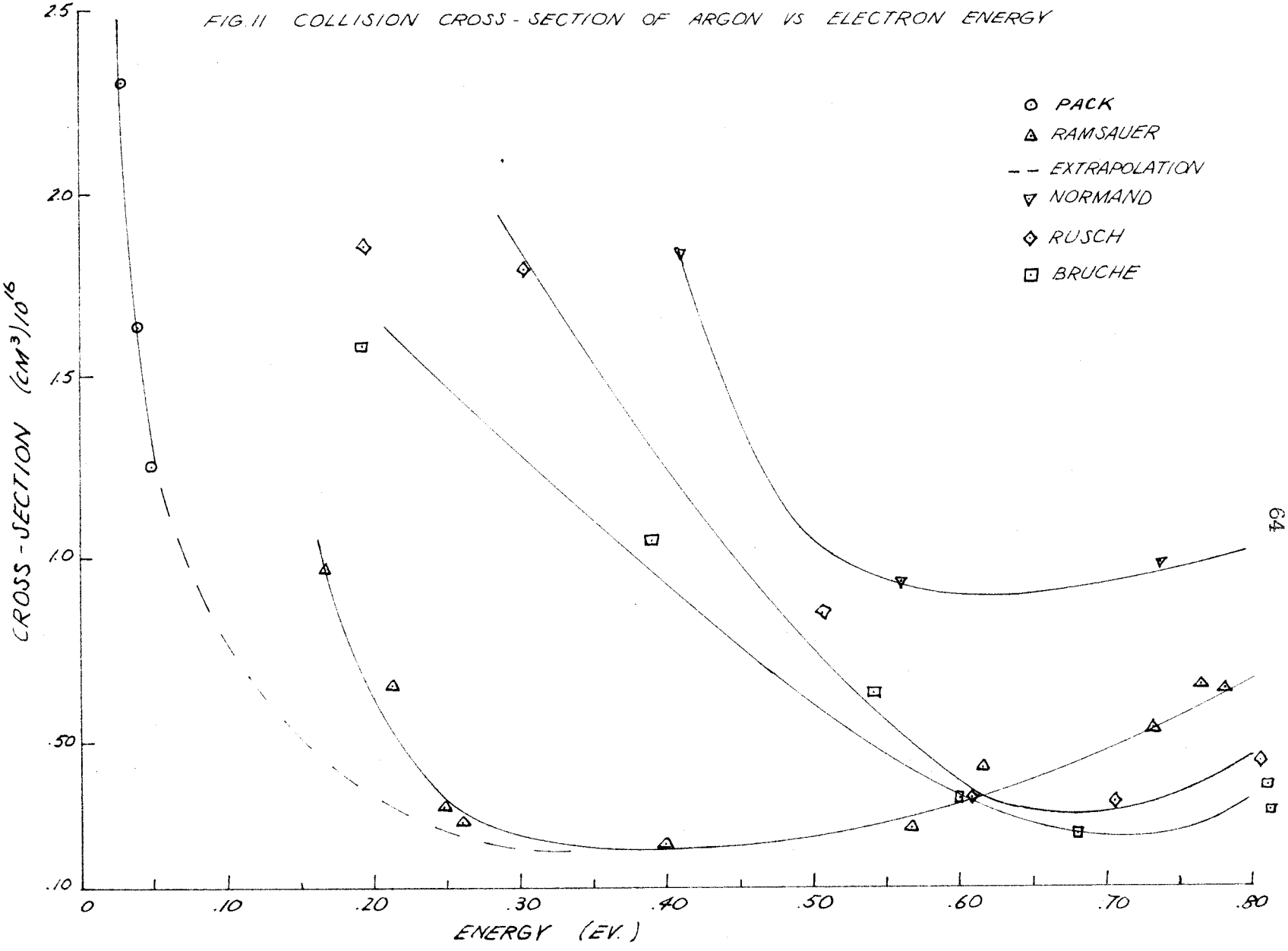

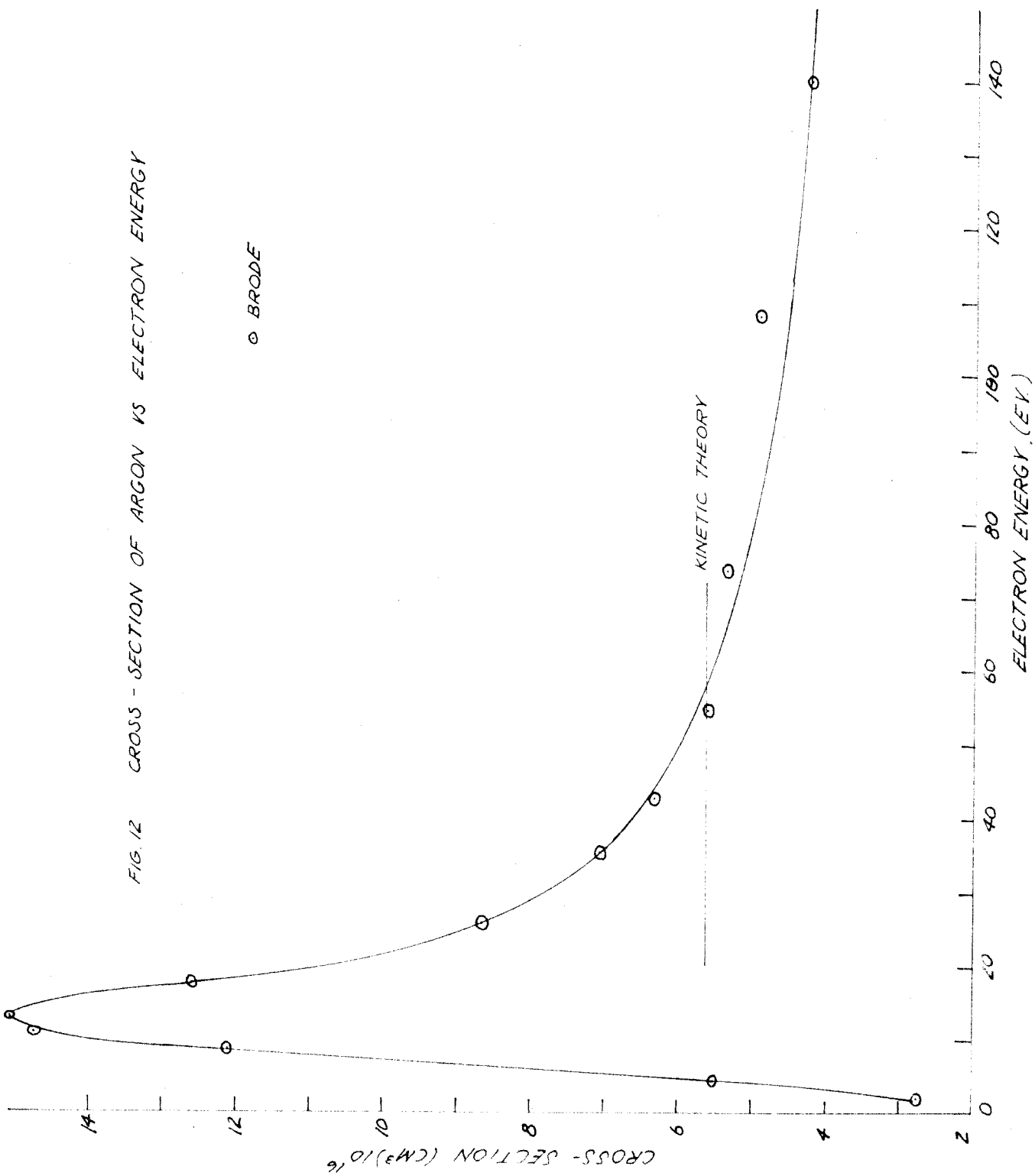
FIG 12 CROSS - SECTION OF ARGON VS ELECTRON ENERGY
⊙ BRODE
KINETIC THEORY
CROSS- SECTION (CM²)10⁻¹⁶
ELECTRON ENERGY, (EV.)
0
2
4
6
8
10
12
14
20
40
60
80
100
120
140

FIG. 13 COLLISION / IMPRESSED FREQUENCY RATIO VS MACH NUMBER

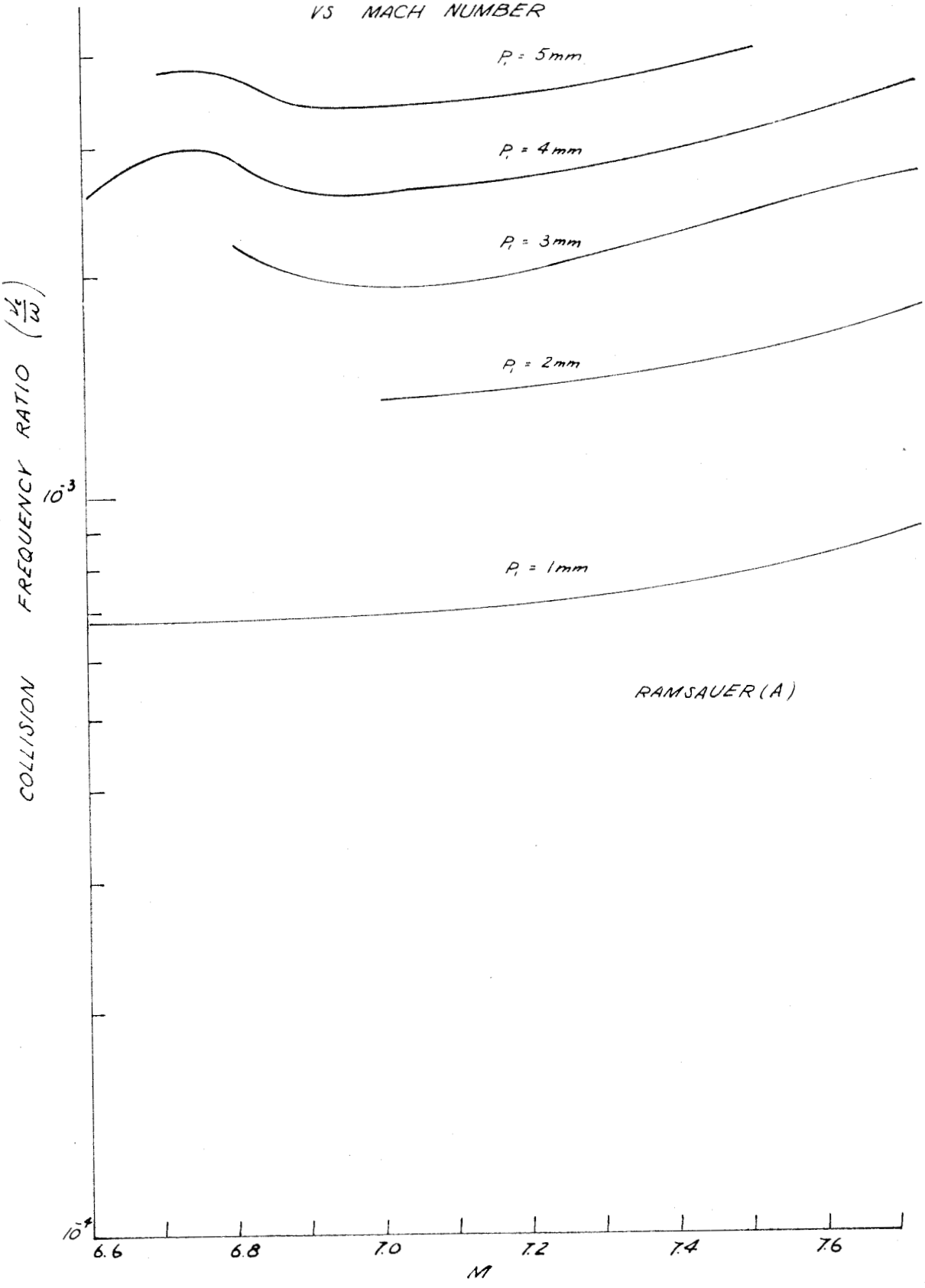

FIG. 14 COLLISION / IMPRESSED FREQUENCY RATIO VS MACH NUMBER

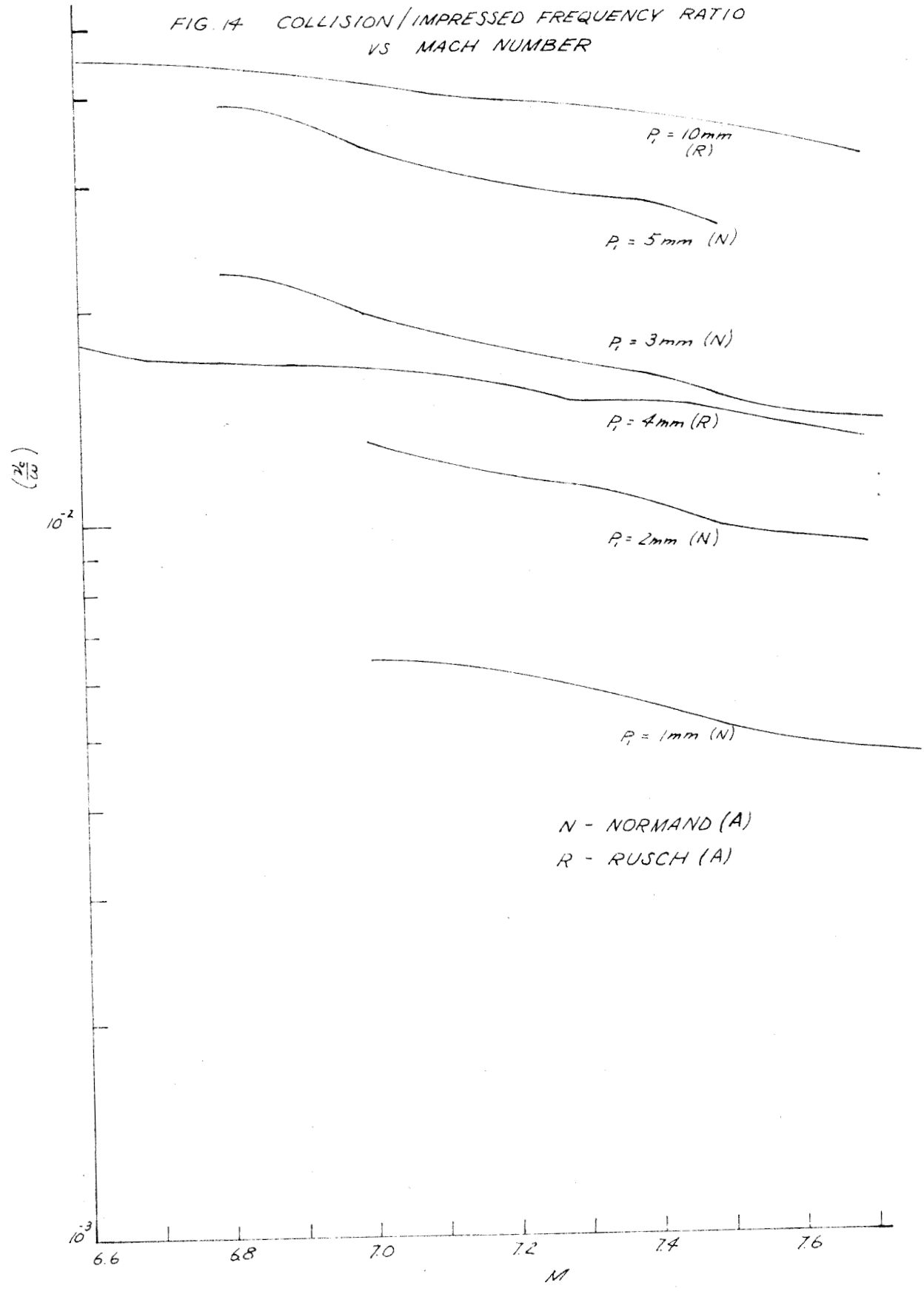

FIG. 15 ATTENUATION VS MACH NO.

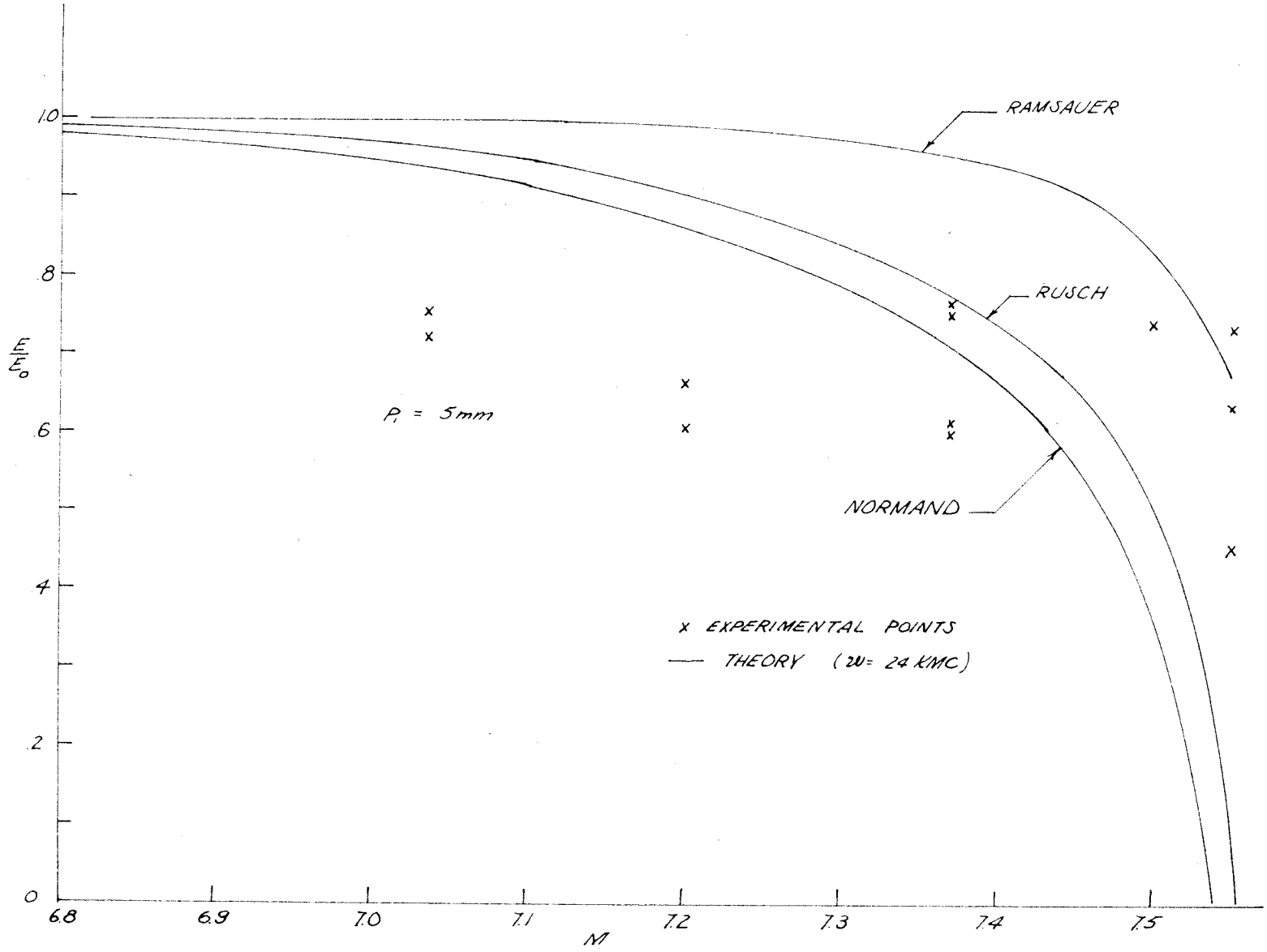

FIG 16 ATTENUATION VS MACH NO.

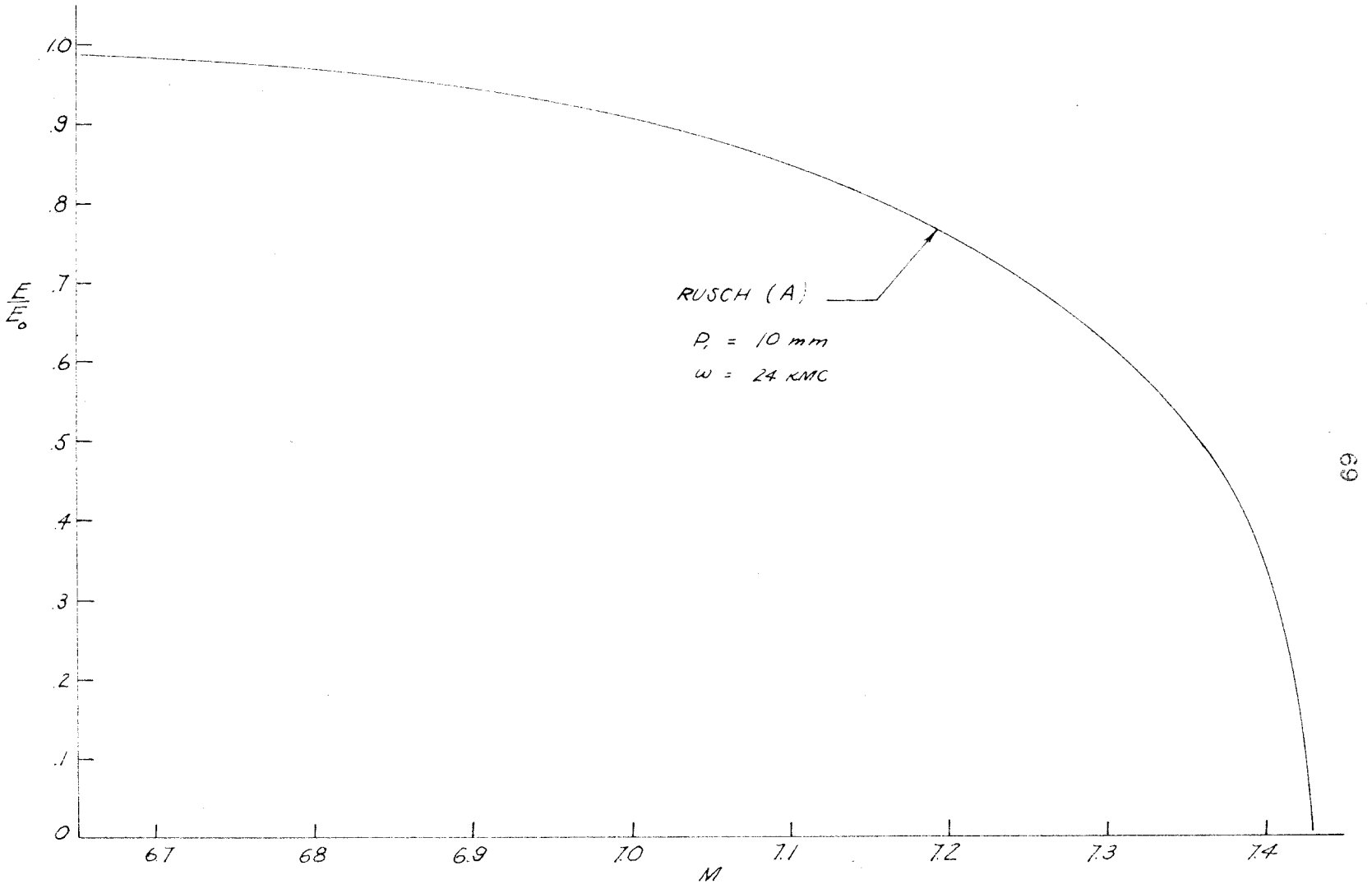

FIG. 17 ATTENUATION VS MACH NO.

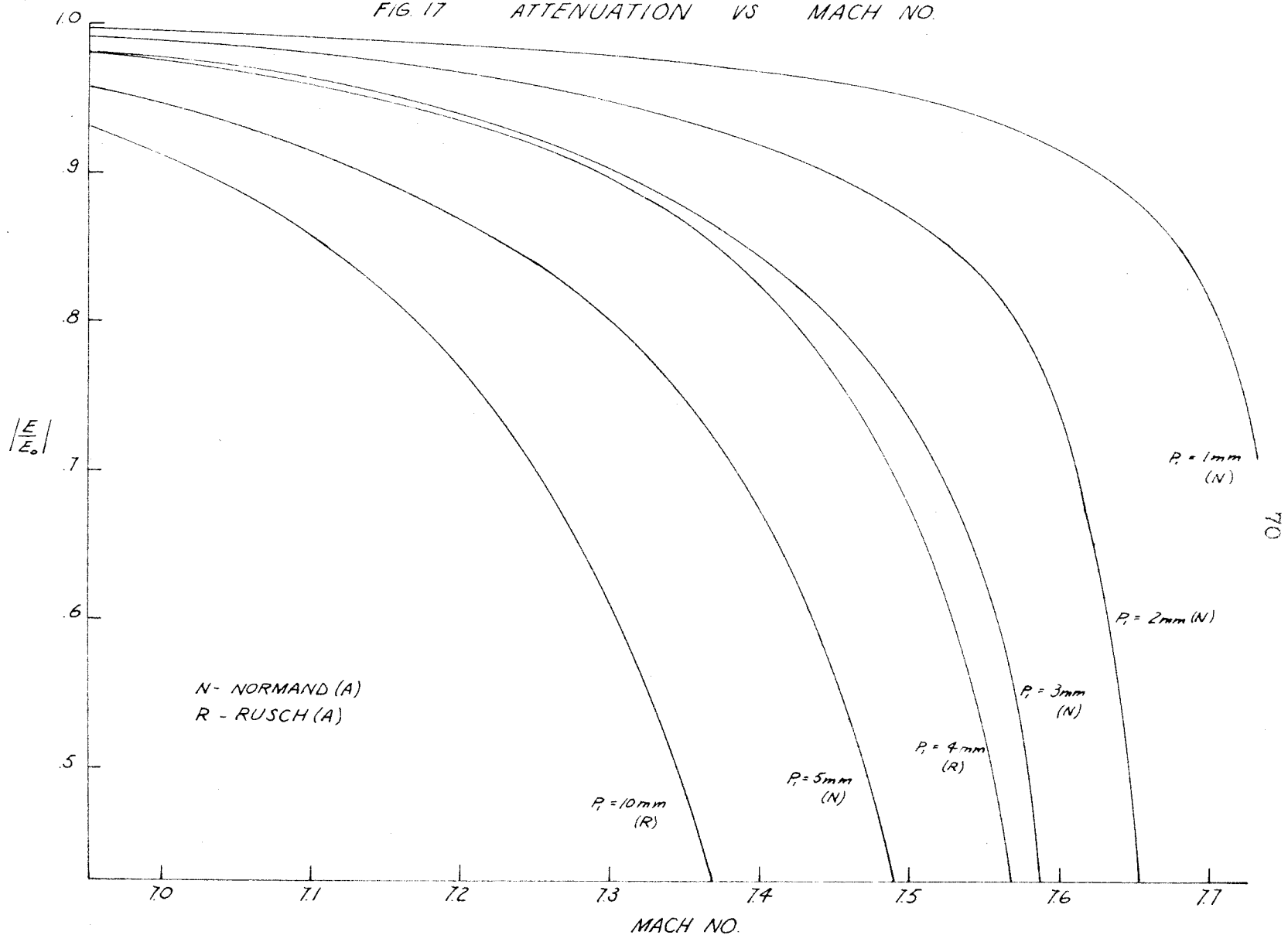

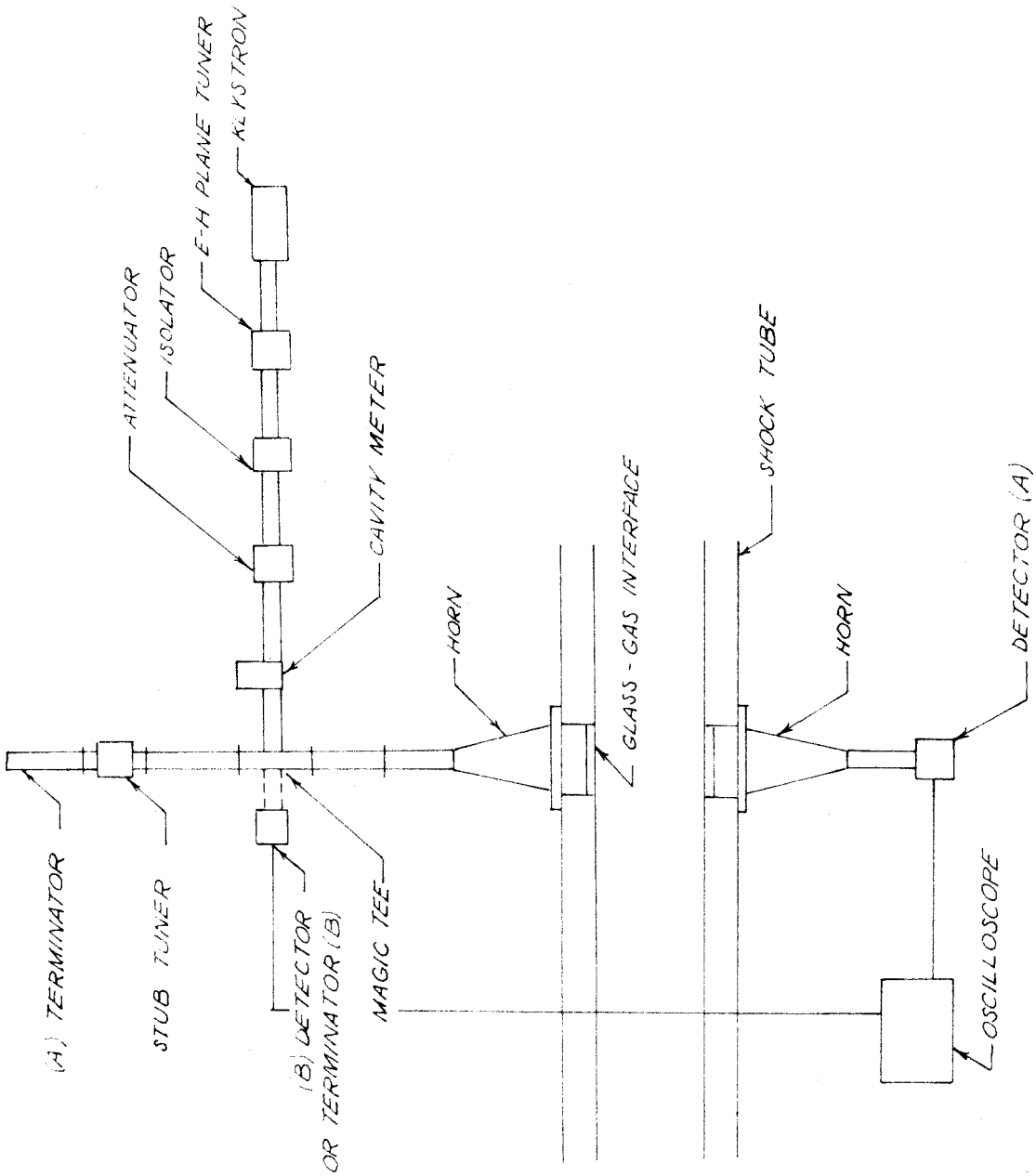

FIG. 18 MICROWAVE NETWORK

FIG. 19 SHOCK TUBE FACILITIES

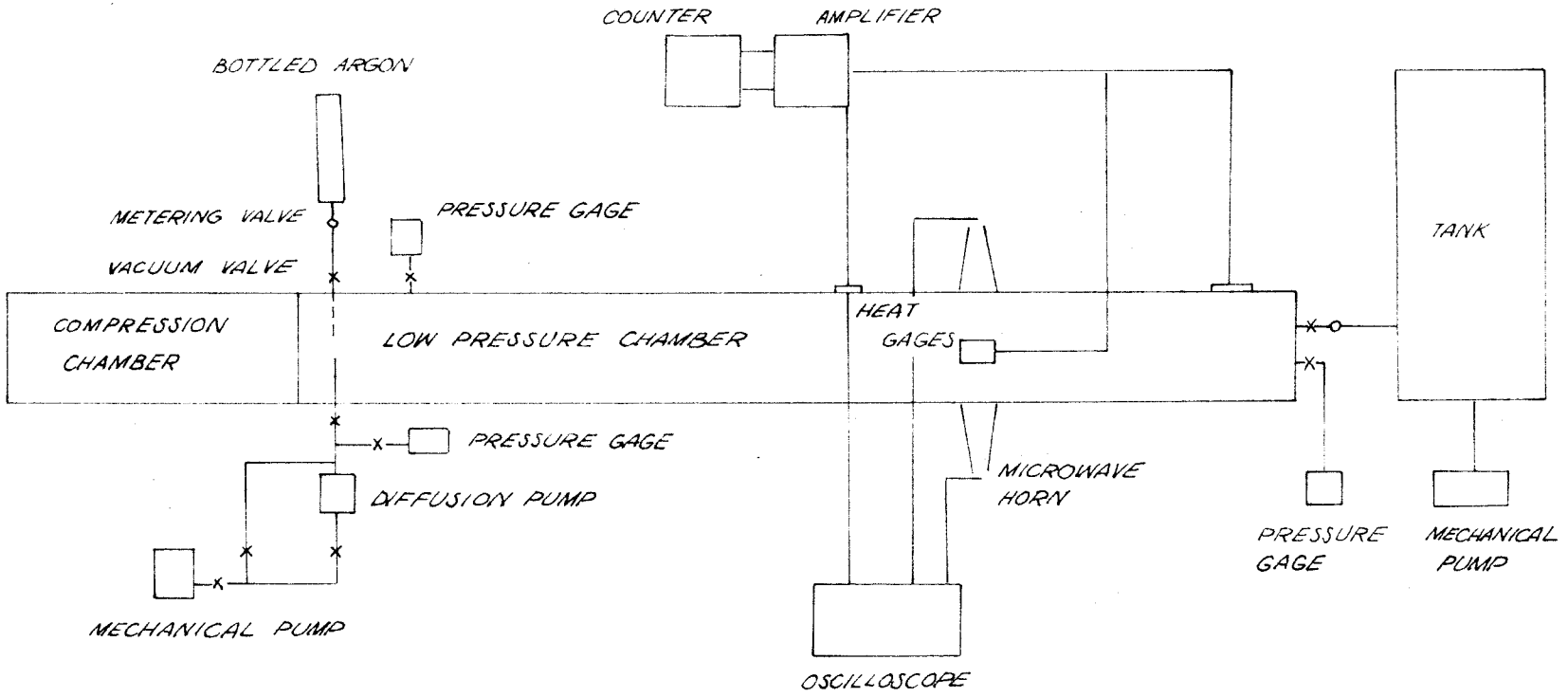

FIG. 20 POWER SUPPLY - KLYSTRON CIRCUIT

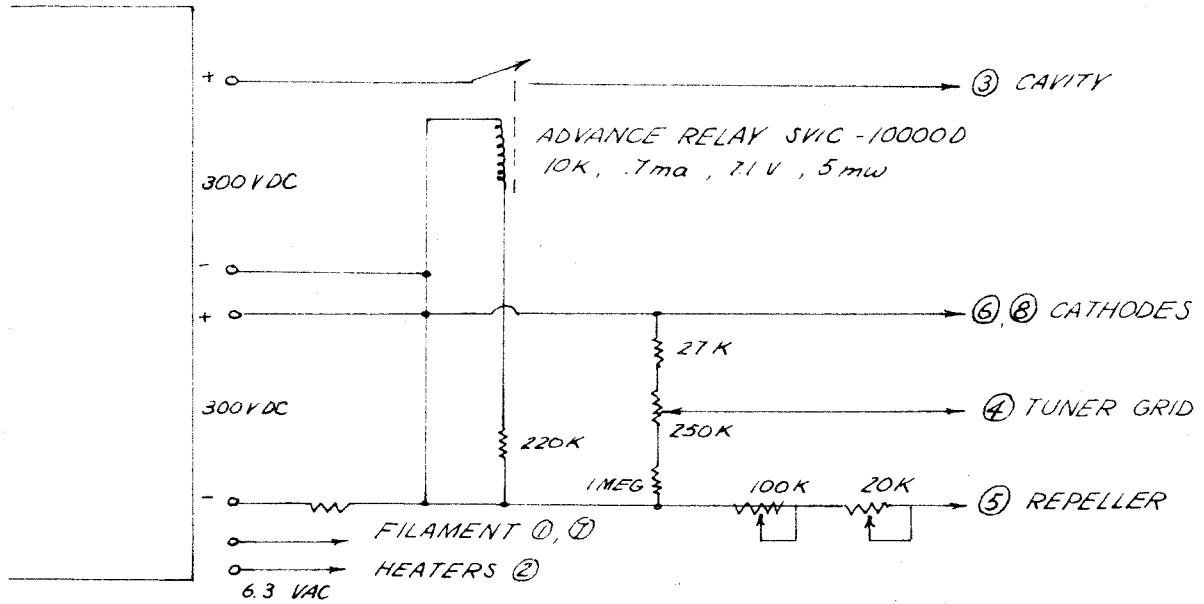

FIG. 21 RELAXATION TIME OF IONIZATION VS MACH NUMBER

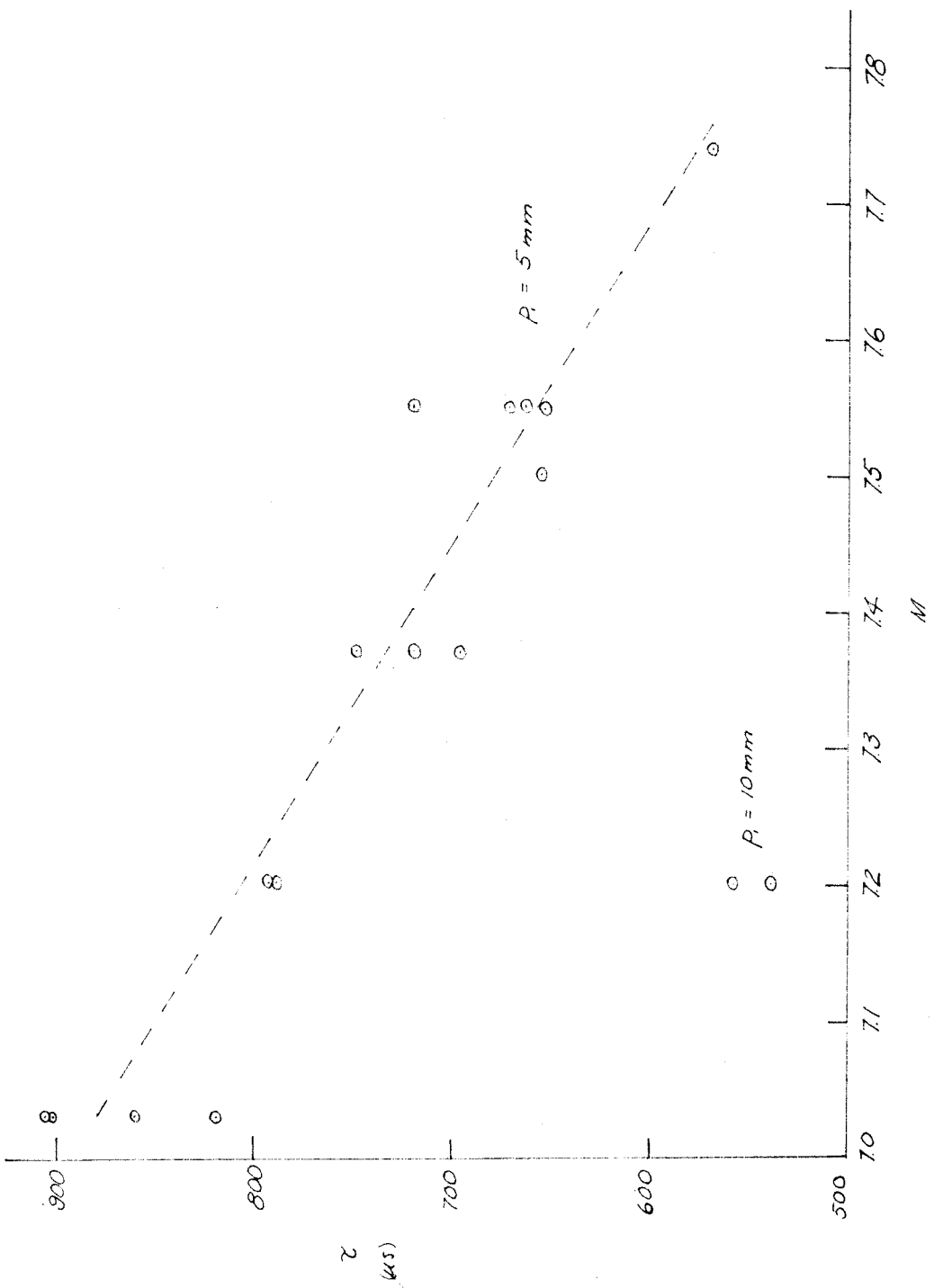

FIG. 22 RELAXATION TIME OF IONIZATION VS RECIPROCAL OF TEMPERATURE BEHIND INCIDENT SHOCK

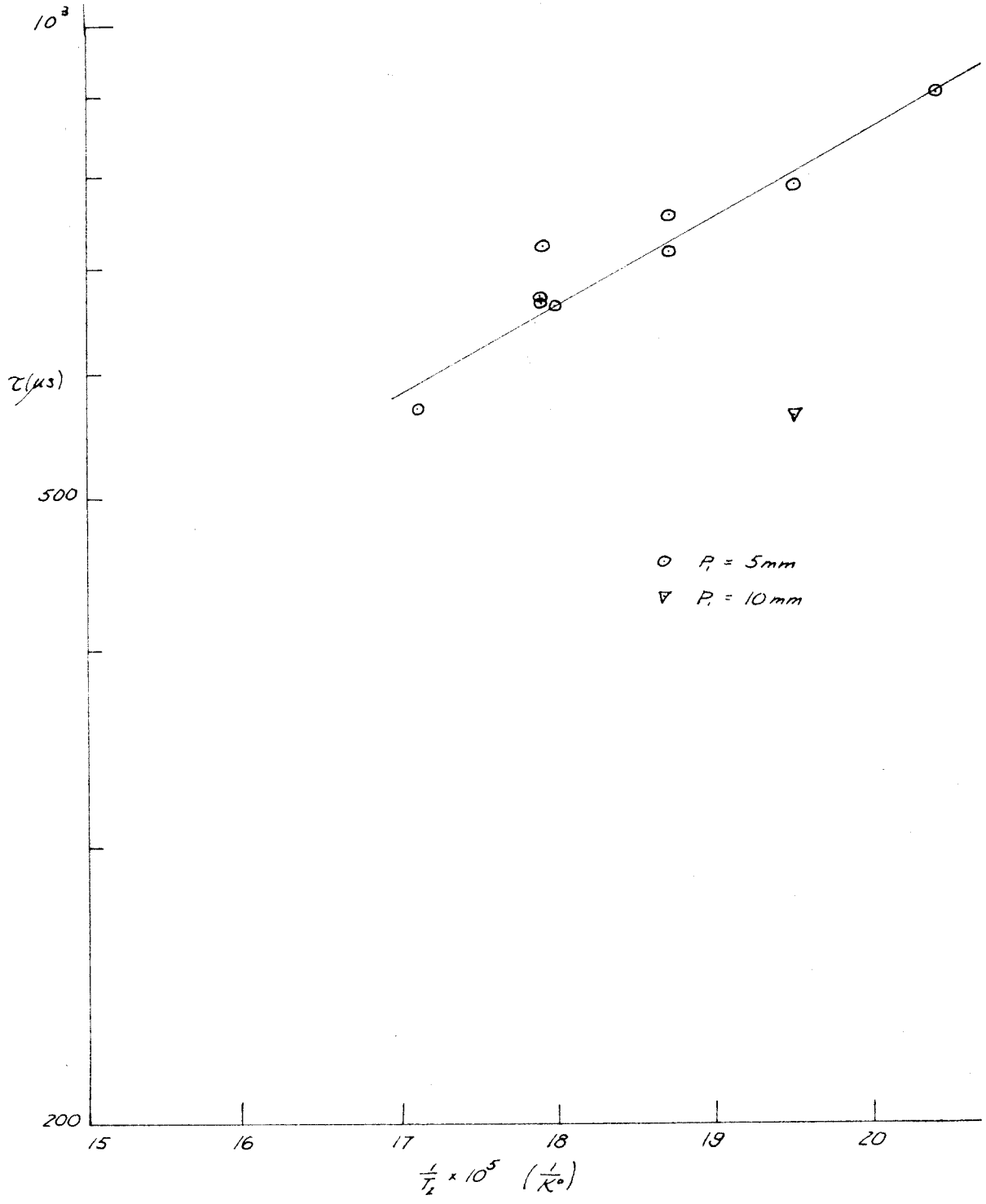

FIG. 23 RELAXATION TIME FOR IONIZATION OF ARGON VS $\frac{1}{T_2}$

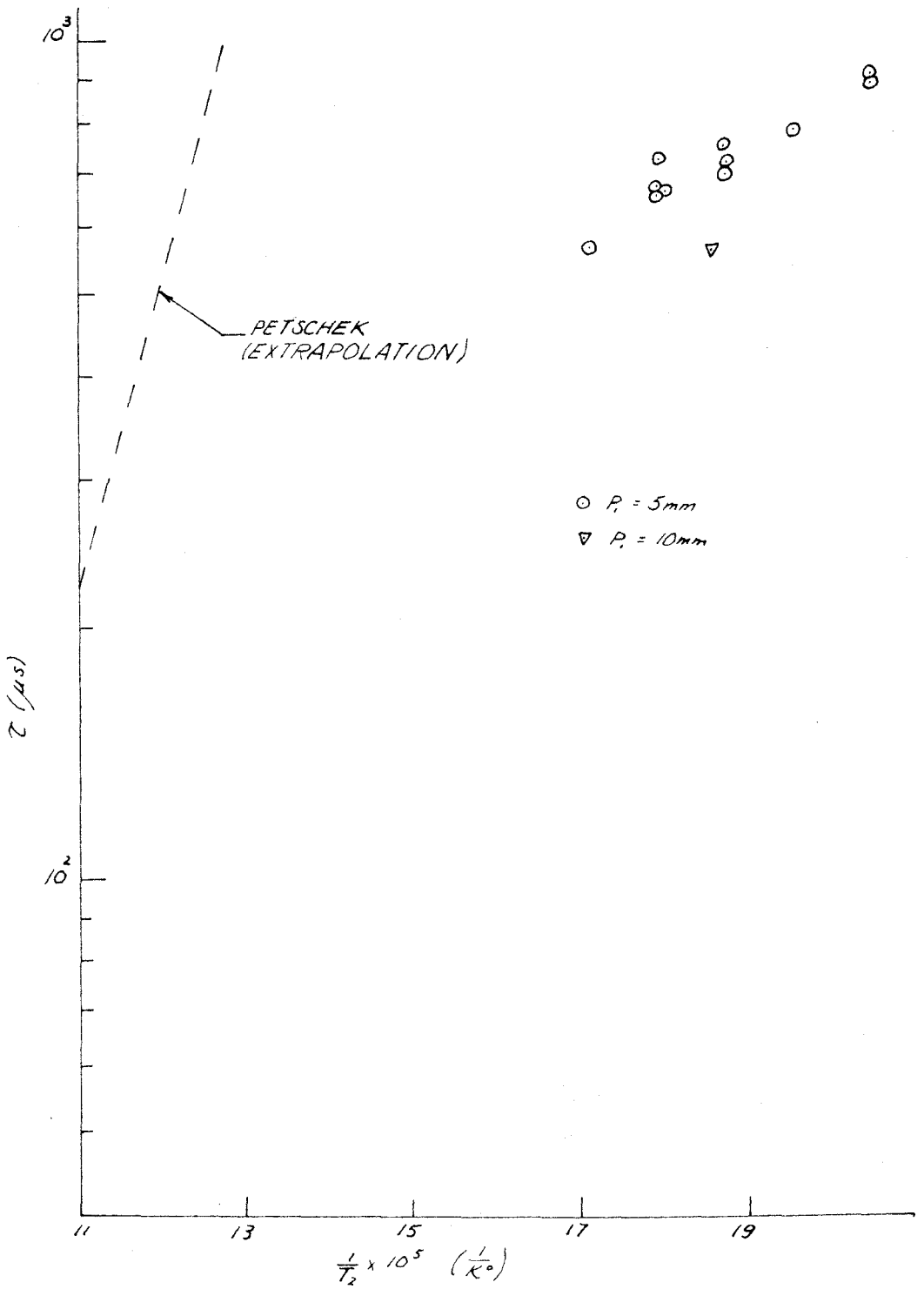

FIG. 24 MICROWAVE TRACES

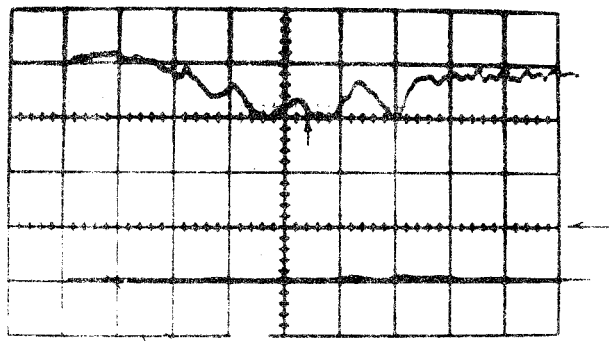

P_1 = 5mm

M = 7.5

SW. RATE = 50 μs/cm

TR = .05 V/cm, RE. = .05 V/cm

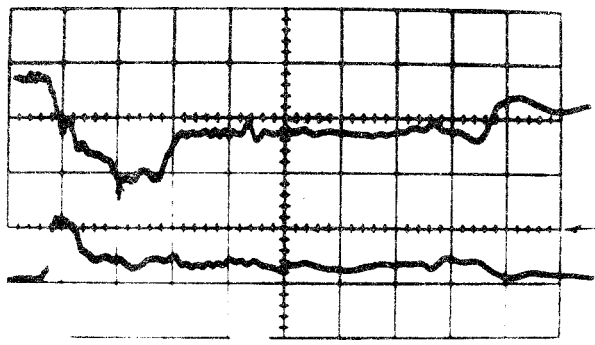

P = 5mm

M = 7.55

SW. RATE = 100 μs/cm

TR = .05 V/cm, RE. = .02 V/cm

MIN. TRANSMISSION

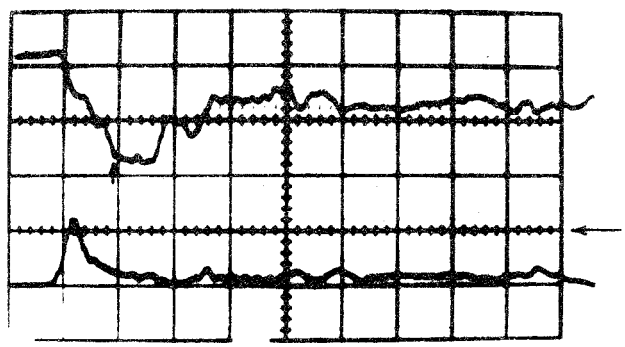

P = 10mm

M = 7.2

SW. RATE = 100 μs/cm

TR = .05 V/cm, RE = .05 V/cm

SYMBOLS

a	speed of sound
A	collision cross-section
B	magnetic induction
C	speed of light
C_p	specific heat at constant pressure
E	electric field
f	partition function
F	Helmholtz free energy
G	Gibbs function
h	enthalpy
J	current density
j	internal partition function
k*	propagation constant
k	Boltzmann's constant (1.38×10^{-16} ergs/^{o}K)
K	equilibrium constant
l	mean free path
m	mass
M	Mach number
n	stoichiometric coefficient
p	pressure
q	charge
R	gas constant (8.31×10^{7} ergs) mole ^{o}K
S	entropy
t	time
T	temperature
U	particle velocity
V	velocity
x	mole fraction
z	path length across tube
β	attenuation factor
ϵ	dielectric constant
ν	stoichiometric coefficient
μ'	chemical potential
λ	obsolete activity
$\mathscr{D}$	statistical weight
W_p	plasma frequency
W	impressed frequency
α	degree of ionization
ρ	density
γ	specific heat ratio
θ	ionization potential
ν_c	collision frequency
μ	magnetic permeability